IMMERSION FREEZING OF NON-PROTEINACEOUS BIOLOGICAL AEROSOL PROXIES & ARCTIC AMBIENT PARTICLES

by

Kimberly M. Cory

A Thesis Submitted in Partial Fulfillment

Of the Requirements for the Degree

MASTER OF BIOLOGY

Major Subject: Bioaerosols

West Texas A&M University

Canyon, Texas

May 2019

ABSTRACT

Ice-nucleating particles (INPs) are particulates that initiate atmospheric freezing in the temperature range between 0°C and approximately -40°C. Bioaerosols are organic materials, such as bacteria, plants, fungi, and/or archaea, that are dispersed into the atmosphere, in solid or liquid phase, causing ice to form at temperatures as high as -1°C. These particles play an important role in climate science because they alter microphysical properties of a cloud and chemical composition of cloud particles and precipitation. However, the research done on INPs has overlooked the potential for biological influences. There are many sources from which these bioaerosols can come; for example, the aerosols can come from the ocean through the bubble bursting process, river and lakes, areas plagued with drought and heavy winds, or even within the snow in regions that coincide with low temperatures. This study attempted to close that gap in knowledge by researching the ice nucleating capabilities of cellulose and particles collected in the world's northern most town.

The first study is the laboratory-based study to characterize ice nucleation efficiencies of several different cellulose samples, and whether the ice nucleation efficiency is dependent on the physical size of the particle. For cellulose, the project focused on nine laboratory-generated samples that were used as proxies to generate a solution that allowed no interference from other cellulose samples. The nine samples were grouped into two categories, normally microcrystalline (Microcrystalline Cellulose, Fibrous cellulose, α-cellulose, and Arbo-cellulose) and nanocrystalline (Nanocrystalline cellulose, 2,2,6,6-tetramethylpiperidine-1-oxyl Cellulose Nanofibers short length, 2,2,6,6-tetramethylpiperidine-1-oxyl Cellulose Nanofibers standard

length, Carboxymethylation Cellulose Nanofibers gel, Carboxymethylation Cellulose Nanofibers powder). To test ice nucleation efficiency, the experiments were run on a Cryogenic Refrigerator Applied Freezing Test (CRAFT) at the National Institute of Polar Research (NiPR) and at West Texas A&M University (WTAMU). In the cellulose project, the results showed that the microcrystalline cellulose did not have a clear distinct difference in ice nucleation as compared to the nanocrystalline. This indicated that the ice nucleation efficiency was not dependent on the size of the particle, which opposes the previous observation that the microcrystalline cellulose is more active than the nanocrystalline cellulose materials. For the future studies, a wider variety of cellulose samples needs to be tested to further increase the amount of data available for the atmospheric model, such as the Global Forecast System. This may enable researchers to stimulate what will occur within the atmosphere with a known amount of a specific concentration. Another step needed is a comparison study between laboratory generated cellulose samples and naturally collected cellulose samples that are ambient within the atmosphere.

The second project focused on samples collected in Ny-Ålesund, Svalbard, to study the ice nucleation efficiency of suspended particles. There was a total of ten nucleopore filters collected over the period of the entire month of March in 2017. The significant findings in the Arctic project was that there was bimodal ice nucleation, which indicates that there are marine biogenic aerosols coming off the marine microlayer, behavior well matched with the previous marine microlayer results. For further research, samples should be collected during other seasons to determine whether these samples are just seasonal or a year-round occurrence. Another study should also focus on what specifically is occurring with the marine biogenic aerosols to determine what is happening between the atmosphere and the

ocean. All of these advances would help to further understand what is happening to the atmosphere and how the scientific community could further determine what will occur when the concentrations of specific particulates are known.

ACKNOWLEDGMENTS

I would like to express my gratitude to Dr. Naruki Hiranuma, my major research advisor and mentor, for his guidance, encouragement, and patience throughout the course of my research at West Texas A&M University. I am indebted to him for providing me the many opportunities that this project has provided, and the growth in my research capabilities that it has allowed.

I would also like the thank the members of my thesis committed for their support and guidance: Dr. Jim Rogers and Dr. David Sissom. I would especially like the thank Dr. Yutaka Tobo for his time, guidance, and kindness while mentoring me while abroad and stateside. To the late Dr. Rocky Ward, I would like to express my appreciate for all the help and guidance he provided in the continued growth of my education. He will be missed.

I am grateful to my fellow students and peers for their assistance in completing these projects: Craig Whiteside, Maria Pantazi, Kotaro Murata, and Joshua Mills.

Lastly, my deepest appreciation to my grandmother, Dr. Kathleen W. Stamback, for her continued guidance even after her passing. Without the work she set down in her research, I would not have been able to set the ground work for my own endeavors in the research community. May I continue to make you as proud as you have made our family.

Approved

[Co-Chairman, Thesis Committee] [Date]
Naruki Hiranuma

[Co-Chairman, Thesis Committee] [Date]
William J. Rogers

[Co-Chairman, Thesis Committee] [Date]
David Sissom

[Department Head/Direct Supervisor] [Date]

[Dean, Academic College] [Date]

[Dean, Graduate School] [Date]

TABLE OF CONTENTS

LIST OF FIGURES AND TABLES

TABLES

FIGURES

CHAPTER I

INTRODUCTION

1.1 Atmospheric Ice Nucleation

In the mid-latitude and polar regions, the mixed-phased clouds contain both liquid and frozen water, hence the name (Hoose et al., 2008). Within the mixed-phase clouds, ice will form through the processes of homogeneous and heterogeneous ice nucleation (Hartmann et al., 2011). Homogenous ice nucleation occurs without a foreign substance initiating the process; thus, it represents pure water freezing (Hartmann et al., 2011). Heterogeneous ice nucleation, on the other hand, has ice formation induced by a foreign substance (Hartmann et al., 2011). These foreign substances can consist of natural and/or anthropogenic particles, referred to as ice-nucleating particles (INPs), that can initiate the formation of ice at temperatures higher than about -40°C and act as ice embryos (Christner et al., 2008). Primary aerosols that can be emitted into the atmosphere can come from oceans, deserts, volcanic eruptions, or vegetation debris, while secondary aerosols are created from gas-to-particle conversion from volatile organics (Kanji et al., 2017). Some examples within the atmosphere are black carbon, which have an average long-term concentration of 0.99 ± 0.02 μg m^{-3} (Dumka et al., 2010), and mineral dust coming from the coasts of Africa, which have a concentration of < 5 μg m^{-3} [excluding the summer months] (Prospero, 1999). INPs impact both the hydrologic cycle and radiative properties of clouds due to their being the primary triggers for ice and

precipitation formation (Hiranuma et al., 2015). It still remains unclear which compound nucleates ice, but the candidates include carbohydrates and oxidized polymers (Hiranuma et al., 2015).

1.2 IN & Bioaerosols

The glaciation of the atmospheric clouds is important because of its effect on the cloud and precipitation formation and the Earth`s energy budget (Boucher et al., 2013). Ice nucleation causes an increased number of droplets to occur within the fixed cloud water content which increases the cloud albedo, thus effecting the Earth`s budget (Hoose et al., 2008). Bioaerosols are organic in nature and cause freezing above -1°C (Després et. al., 2012). One organic source comes from the marine microlayer and is estimated to be 10 ± 5 Tg yr^{-1} or the primary organic submicrometer aerosols from around the world (Wilson et al., 2015). The way these samples are emitted into the atmosphere is through the bubble bursting effect, which lofts the material with a mixture of organics and sea salt (Wilson et al., 2015). Some other sources of biological material that have been found in the clouds are plant-associated bacteria, fungi, algae, and pollen (Christner et al., 2008). For the bacteria like *P. syringae*, there is an ice nucleation active protein, 120- to 180-kDa, on the outer membrane, and this protein is made up of a repeated structure of octapeptide (Christner et al., 2008). This protein allows for the binding of water molecules in a particular order that enhances the ice crystal formation in a way of a template (Christner et al., 2008). In bioaerosols, it has recently been seen that particulates with a size ~10 nm have the capability to separate from the fungal spores, pollen, or even marine organic aerosols, and that these single particulates can initiate heterogeneous

ice formation (Kanji et al., 2017). These specific particles can also bind to a host, such as mineral or soil dust, to disperse into the atmosphere, and may provide the needed chemical bond to stabilize ice nucleation but makes detection more difficult (Kanji et al., 2017).

1.3 Aerosol-cloud Interactions

Aerosol particles that are found within the mixed-phased clouds have two ways of potentially effecting the cloud and its formation and other properties. The first effect is the "direct" effect where said particles will scatter and absorb the solar and thermal radiation that is attempting to pass through the cloud. In comparison, the "indirect" effect is separated into two categories: (1) aerosol particle concentration increasing with the cloud droplet effective radius decreasing causing higher cloud albedo; (2) inhibition of precipitation and increase of cloud water caused by the decrease in the cloud droplet effective radius (Takemura et al., 2005).

For instance, particles like sulfate and carbonaceous aerosols have a direct effect on the climate system through the physical mechanisms (Lohmann & Diehl, 2006). To start, the particles will scatter and absorb solar radiation and emit any of thermal radiation. At the surface level, the net reduction for shortwave radiation for all aerosol direct and indirect effects is ~ -1.8 and -4 W m^{-2} (Lohmann & Diehl, 2006). Further, the aerosols can also act as cloud condensation nuclei or INP, which can be <50 nm diameter of primary or secondary particles with the accumulation of secondary organic compounds (Kerminen, 2001; Lohmann & Diehl, 2006). This will also reduce the precipitation efficiency within the high temperature clouds, which ends up increasing the cloud lifetime (Lohmann & Diehl, 2006).

1.4 Types of Freezing

There are four major paths of heterogeneous ice nucleation in the atmosphere. The first mode is deposition nucleation where ice is formed when water vapor deposits onto a solid surface (Murray et al., 2011). Deposition freezing is thought to be of lesser importance than condensation and immersion freezing (Lohmann & Diehl, 2006), but may be of importance to ice clouds in the upper troposphere (DeMott, 2002). For example, deposition freezing temperatures have been seen for kaolinite with an onset of -19°C with a supersaturation level of 20% (Lohmann & Diehl, 2006). The second mode of freezing is condensation freezing where ice nucleation occurs when water condenses onto an INPs while cooling (Welti et al., 2014). Contact freezing is the third mode where a particle comes into contact with a supercooled droplet cause ice formation (Murray et al., 2011). Lastly, the fourth mode is immersion freezing which consists of typically insoluble particles immersed in a supercooled droplet causing ice formation above -38°C (Koop et al., 2000). Contact and immersion freezing are thought to be the two most important modes of freezing within the mixed-phased clouds (Murray et al., 2011). Of the two most important, immersion freezing is believed to be the more dominant mode (Tobo, 2016).

1.5 Cellulose

Cellulose is an important biological INP due to the fact that it makes up fifty percent of a plant as the structural component of the cell wall and is the most abundant organic molecule (Quiroz-Castañeda & Folch-Mallol, 2013). By linking thousands of unbranched, parallel D-glucopyranose units by β-1,4-glycosidic bonds, it creates natural cellulose with two different types of polymers [crystalline and linear]. To create microfibrils, the cellulose chains consist of twenty-five to thirty-six chains, and the glucose molecules in those chains are rotated by 180°, with the cellobiose as

the repeating unit, to create the crystalline cellulose (Quiroz-Castañeda & Folch-Mallol, 2013). Fibers of cellulose can be found in leaves, bark, and the stems on woody vegetation. This shows the significance of the concentration measured of cellulose in an urban area, which was from the plant debris at or near ground level (Hiranuma et al., 2015). The measured mass concentration in the 2015 report was > 1 $\mu g\ m^{-3}$ (Hiranuma et al.). From these concentrations, it shows that cellulose might be comparable to other known particulates due to its high concentrations.

In this study, nine different types of laboratory generated cellulose of varying sizes were compared: four microcrystalline cellulose and five nanocrystalline cellulose. The four microcrystalline were 1) Microcrystalline Cellulose (MCC; Aldrich, 435236), 2) Fibrous Cellulose (FC; Sigma, C6288), 3) α-Cellulose (Sigma, C8002), and 4) Arbo Cellulose (JR Rettenmaier & Söhne, ARBOCEL). The five nanocrystalline cellulose were 1) 2,2,6,6-tetramethylpiperidine-1-oxyl Cellulose Nanofibers short length, 2) 2,2,6,6-tetramethylpiperidine-1-oxyl Cellulose Nanofibers standard length (TEMPO-CNF; Nippon Paper Industries), 3) Carboxymethylation Cellulose Nanofibers gel, 4) Carboxymethylation Cellulose Nanofibers powder (CM-CNF; Nippon Paper Industries), and 5) Nanocrystalline Cellulose (NCC; Melodea, WS1). The strand of cellulose fibers varies in their length from 100 nm to > 100 μm, which were used to investigate in the size dependency. The hypothesis was that the shorter particulates would be more IN active than the longer strands.

1.6 Arctic

Within the Arctic, there is an occurrence called the Arctic amplification – where, in comparison to the global average, the region has warmed over twice as fast – this warming occurs year-round but is most prominent in autumn and winter (Cohen et al., 2014). There are believed to be many reasons that the Arctic amplification is

occurring and getting worse as time progresses. Initially, Arctic amplification was thought to have been caused by the melting of the reflective snow (46% in June) and ice cover which lead to the exposure of darker surfaces that would absorb rather than reflect, thereby leading to the further retreat of the snow and ice (Serreze & Barry, 2011). More recently, the retreat of the ice covering the Arctic sea, which is 11.5% per decade since 2010, has been noted to alter the heat fluxes between the atmosphere and Arctic ocean (Serreze & Barry, 2011). Another reason the amplification is occurring is the change in water content and cloud coverage which would have an effect on the downward longwave radiation flux (Serreze & Barry, 2011). The reason for this is because the net all-wave radiation flux tends to be higher in the presence of cloud coverage, also known as heat absorption (Serreze & Barry, 2011). This causes higher air temperatures to occur and sends stronger longwave radiation back to the surface. These factors combined, will bring the spring melt to occur sooner or last longer (Serreze & Barry, 2011). The Arctic region has a balanced annual mean of heat flux convergence through the loss of longwave radiation to space, but with the excess particles causing that to no longer occur, this will affect the sea ice extent and surface albedo (Serreze & Barry, 2011).

To explain where those particulates are coming from, modeling studies have suggested that a dominant source is the ocean when dust concentrations are low (Irish et al., 2017). Wilson et al. (2015) states that the organic aerosols are ejected into the atmosphere through bubble bursting effect when the sea-spray has similar organic compositions as the sea surface microlayer. The Arctic is a region to study for INPs because the atmospheric concentrations in this region have been found to be sensitive (Irish et al., 2017). Another reason is because the scientific knowledge of aerosol-cloud interactions, in regard to contribution, in the Arctic continues to remain scarce.

1.7 Objective

The investigation of cellulose and arctic filter samples was initiated to gather more knowledge about INPs in both lab and field settings. For the cellulose project, the study focuses on the impact potential between several biological aerosol surrogates in laboratory-measured freezing capabilities. This study is important because there is little research regarding bioaerosols, so identifying some biological INPs will allow for a better understanding of the effects those aerosols have on ice formation within mixed-phase clouds. As for the Arctic project, the study focused on identifying some of the Arctic INPs and how those particles interact with water vapor and supercooled water droplets in the missed-phased clouds in the Arctic. The scientific knowledge of the aerosol-cloud interaction on the Arctic amplification is scarce, so this project will contribute new knowledge. Both projects will help in the understanding of particle cloud interaction within mixed-phased clouds.

CHAPTER II

LITERATURE REVIEW

2.1 Ice-Nucleating Particles – (Kanji et al., 2017)

Primary aerosol particles are generally emitted into the atmosphere through natural sources, such as volcanic eruptions, deserts, oceans, vegetation debris. The important anthropogenic sources of atmospheric aerosols come from transportation, industrial processes, deforestation, biomass burning, and agricultural practices. Secondary aerosol particles result from got-to-particle conversion of volatile organics. Biological aerosols are airborne bacteria, fungal spores, phytoplankton, lichens, pollen, marine exudates, and plant fragments. These aerosols are IN active, but they are all dependent on the type of particle and their relevance to the atmosphere is dependent on the concentration levels.

Mineral dust is considered the most important INP type because of their effective ice nucleating ability and has an emission rate of up to 5000 Tg yr^{-1}. The main source of dust particles are arid soil or deserts, volcanoes, and agricultural soils. These particles have activation temperature of < -15°C. They can activate at higher temperatures depending on the amount of K-feldspar fraction, particle concertation per droplet (immersion mode), and particle size. Not only can these particles be found in regional atmospheres, but they can withstand long range transport. It is the most representative particle collected in orographic wave clouds and cirrus clouds in the upper troposphere.

The organic material found in secondary aerosol particles can be emitted by marine organisms and collected from the sea surface microlayer. These were found to nucleate ice through deposition mode when the RH_i < 120% at -40°C and temperatures as warm as -10°C in immersion mode. For the land secondary organic aerosols collected in Mexico, the samples were found to activate at temperatures less than -33°C and RH_i of ~130%. This shows that these samples are extremely varied due to their complex mixtures of organics.

On the other hand, bioaerosols have been found in the ice residues sampled from clouds, but their impact on cloud formation is unclear on a regional and global scale. These particles are found to have and ice nucleation protein (inaZ), which is found on the outer membrane of *Pseudomonas syringae bacteria*. This protein has a unique hydrophilic-hydrophobic pattern that promotes the ordering of water molecules within a nearby vicinity, which enhances ice nucleation. These particles freeze at very low supercooling temperatures (> -15°C). Other bioaerosols, such as marine diatoms, diatom exudates, fungi, and washing waters from pollen, all have ice activation at temperatures less than -15°C.

Soil dust particles are emitted from grazed and agricultural lands and are believed to make up 25% of the global dust emissions. They are seen to have nucleated ice with the same effectiveness as bioaerosols and feldspar samples. The onset temperatures were seen as high as -6°C with concentrations of 0.01 L^{-1}. This is higher than that of natural dust or clay particles when at the same concentration of 0.01 L^{-1} and were found to have onsets of -12°C and -25°C, respectively. These high activation abilities are from the internal mixing of organic material present in the soil particles.

Fossil fuel particles come from the combustion process and emit large quantities of chemically complex particles. These are placed into two groups: (1) Carbonaceous matter formed by pyrolysis of the fuel molecules, and (2) ash particles that are derived from noncombustible constituents in the fuel and form heteroatoms in the original organic molecular structure. Biomass burning particles are derived from ash and smoke from agricultural and forest fires, wood stoves, heating, and industrial activities. These particles may be playing an important role in the formation of ice clouds due to their high emission rates and have a higher concentration. In the immersion freezing mode it is found that these types of particulates freeze around -12°C to -36°C. For example, Alaska reported an average concentration of 1 L^{-1} at -18°C.

Volcanic ash is seen to be emitted at a rate of ~13 Tg yr^{-1} but can be higher if an explosive eruption takes place. These particles are seen to act as INPs at temperatures ranging from -13°C to -23°C. Not only were they active in immersion mode, but they were found to behave as active INPs in contact freezing (~-8°C). Volcanic ash is seen as more important at colder temperatures and would be of importance with the absence of other more effective particles, such as mineral dust. Lastly, crystalline salts will dissolve and can be emitted into the atmosphere by way of the oceans. They will crystallize by the process of efflorescence or gas-to-particle conversion. These soluble salt particles with a diameter > 25 μm can induce contact freezing at warm temperatures (-7°C). The ice nucleating ability of ice mixed with salts is still unclear.

2.2 Bioaerosols – (Christner et al., 2008)

The most studied bioaerosol with ice nucleating activity are plant associated bacteria (*Pseudomonas syringae, Pseudomonas viridiflava, Pseuromonas fluorescens,*

Pantoea agglomerans, and *Xanthomonas campestris*), fungi (*Fusarium avenaceum*), algae (*Chlorella minutissima*), and birch pollen. *Pseudomonas syringae* and *F. avenaceum* both have been detected in atmospheric aerosols and clouds. Biological IN were found in precipitation from a range of global location at mid- to high-latitude with the most active IN at temperatures greater than -10°C. Few other naturally occurring particles in the atmosphere have onset activation at such warm temperatures, but they would have no noticeable change in activity after heat treatment.

Snow samples taken from France and Montana contain similar average concentration of biological ice nuclei active at temperatures greater or equal to -9°C with 55 and 54 ice nuclei L^{-1}, respectively. Louisiana rain had a high value of 110 ice nuclei L^{-1} but the results were only statistically significant between Montana and Louisiana ($P = 0.04$). The heat treatments eliminated all IN active at temperatures greater than or equal to -9°C in 69-100% of the snow and rain samples, which was the lysozyme-sensitive bacteria.

Over half the rain and snow samples had ice nuclei active at temperatures greater than or equal to -5°C and all were active at temperatures warmer than -10°C. Due to the heat treatment, it was found that 95% of the ice nuclei were active at temperatures warmer than -10°C and could be inferred as proteinaceous, thus, biological in origin. Since all of the samples were sensitive to lysozyme, the samples originated from sources like plants, fungi, and/or archaea. Despite the difference in local ecosystems, the concentrations of ice nuclei at -7°C in midlatitude snow (3-150 ice nuclei L^{-1}) and Louisiana rain (8-230 ice nuclei L^{-1}) were considered similar. With these high concentrations and distributions within the atmosphere, biological ice

nuclei are more than likely to encounter the appropriate condition to affect the atmospheric process leading up to precipitation.

2.3 Machine Comparison – (DeMott et al., 2017)

In recent years, many new methods of ice nucleation particle measurements have been introduced to the scientific community. This study does an assessment of four offline immersion freezing measurement methods and their comparability. The four methods are the Colorado State University ice Spectrometer (IS), North Carolina State University cold stage (CS), National Institute of Polar Research cryogenic refrigerator applied to freezing test (CRAFT), University of British Columbia micro-orifice uniform deposit impactor-droplet freezing technique (MOUDI-DFT), and a single online method (continuous flow diffusion chamber, CFDC). Not only were the machines compared, but the method of aerosol collection that were used with the designated machines were compared as well.

These techniques for immersion freezing are more likely to be in agreement when the temperatures are warmer than -20°C and $n_{INP}(T)$ that are less than ~ 5 L^{-1}. When at lower temperatures and higher $n_{INP}(T)$, the offline immersion freezing methods, except for MOUDI-DFT, will estimate higher than the online CFDC method with ratios of a few to 10 times. The CFDC activation allowed for the capturing of the majority of the immersion freezing activity in most cases, but the study expects that the CFDC underestimates the n_{INP} to a greater degree than the IS due to the CFDC failing to measure larger aerosols. These IS experiments were conducted with a cooling rate of 1°C in three minutes while the MOUDI-DFT used a much faster cooling rate of 5-10°C a minute. These cooling rates may explain why there may have been a better correspondence between CFDC and the MOUDI-DFT. Although, this cannot explain the bias of temperature-dependent nature between the other immersion

freezing methods and the CFDC, but this is not the only discrepancy between the machines.

The techniques had very good agreement within the uncertainty limits that were obtained under many different conditions for the samples but still had temporal overlap. On the other hand, there could be discrepancies that could approach about two orders of magnitude that are not explainable without incorporating systematic artifacts that were inherent with one or more of the techniques. The larger discrepancy between the machines tend to be at the warmer and colder end of the spectrum or mixed-phase cloud freezing temperatures. On the warmer (> -20°C) end of the spectrum, the sampling statistics and uncertainties are what can dominate the comparisons for the online and offline sampling methods. With the sampling methods for immersion freezing, the use of BioSampler – a glass container filled with liquid that samples are immersed in upon collection – or a filter did not have an effect and could be interchanged and still have similar results.

At the lower temperatures, the IS, CS, and CRAFT were able to measure more INPs than what was detected by the CFDC and MOUDI-DFT. There were potential artifacts or biases that were present in the comparisons of the machines. The CFDC excluded the larger INPs and this was seen in the online instruments, and the CFDC requires correction since it is unable to access full immersion of the particles until there is high relative humidity that can be commonly used when sampling the ambient particles. The study was unable to provide assured conclusions in regard to the source of the discrepancies except that the size biases in the sampling will need to be acknowledged.

2.4 Cryogenic Refrigerator Applied Freezing Test – (Tobo, 2016)

Within mixed-phase clouds, the process of immersion freezing is found to be dominant with a group of water droplets that contain INPs. The Cryogenic Refrigerator Applied Freezing Test (CRAFT) was created to allow for a better way to measure these particulates due to the difficultly in measuring INPs. This challenge is due to the concentration values varying over many orders of magnitude based on the temperature, atmospheric conditions, and geophysical locations. Prior techniques have immersed a particle within a supercooled droplet and then suspended that droplet within a gas, and these techniques are limited in measuring high numbers ($> 1\ L^{-1}$) of INPs. Another technique is to immerse particles in supercooled water droplets on a cold stage. These droplets are sub-/super-microliter sized droplets that will hold multiple particulates and is efficient at detecting highly efficient INPs. A problem that is consistent with this method is that some of these droplets that hold no added INPs end up freezing at temperatures of -25°C or warmer with the majority freezing by -30°C. All these problems may be due to contamination within the droplets or supporting substances. This study made a few simple modifications to determine if the cold-stage method is still viable.

This method starts with spreading a hydrophobic layer between the cold-stage and supercooled droplets with a plastic spatula. These droplets are the pipetted onto a plate with an Eppendorf micropipette. A clean bench was added to avoided contamination of the droplets by any airborne particulates that may come in contact with the droplets. The clean bench had a measured concentration of less than $0.1\ L^{-1}$ with the particles having a diameter less than 0.3 μm. The cold-stage and droplets are then placed within a portable cryogenic refrigerator, which is capable of freezing in the range of 50°C to -80°C with an uncertainty of ± 0.2°C. The plate's temperature is

gauged by a single temperature sensor that is attached to the surface of the cold-stage. During the freezing, all droplets and sensor are monitored through a WEB camera. The top of the cryogenic refrigerator has a plate of acrylic to allow for the WEB camera to view the droplets as well as prevent any further particulates from landing on the droplets. There was no gas entering or exiting the system.

To compare the results of the modified system to other previous systems, the study used Illite-NX and Snomax to determine the viability of this system. The results were compared to different instruments that are involved within the INUIT project. This showed that the setup is able to measure relatively high values of ice nucleation active site density per unit of surface area and is able to detect low INPs of Illite NX ($< 0.1\ L^{-1}$) only comparable since the others are typically unable to measure low values. This simple setup allowed for the observation of immersion freezing to a mostly homogenous freezing for pure water droplets at the super-microliter size (5 μm). The biggest difference this machine has over the other cold-stage based techniques is as simple as the materials used as a cold substrate. The hydrophobic layer may be responsible for preventing the influence of frost growth which could affect the neighboring water droplets.

2.5 Microcrystalline Cellulose – (Hiranuma et al., 2015)

The biological origin within the global emissions can vary from a few per cent to a quarter of the mineral dust emission. These biological INPs influence depends solely on their abundance within the atmosphere. One of these biological INPs is natural cellulose. Cellulose is within many biological cell walls and makes up fifty percent of the dry weight in plants. This is why cellulose is present globally in the atmosphere. Field observations were conducted to determine the prevalence of cellulose in the atmosphere, and it was found to biannually have a concentration of >

16 ng m^{-3} and accounts for more than five percent of the total airborne organic matter by weight during the duration of the year, regardless of the season, remoteness, or elevation.

This study examined the ice nucleation efficiency of two types of cellulose, microcrystalline and fibrous cellulose, that have been extracted from wood pulp. Microcrystalline cellulose particles are comparable to natural dust particles, which are the dominating particle below -15°C. These samples were used as proxies for the cellulose within the atmosphere. A dynamically controlled expansion cloud simulation chamber at the Meteorological Research Institute in Tsukuba, Japan was used to investigate the immersion freezing properties of microcrystalline cellulose. Cloud-chambers are sensitive to the immersion freezing process, and microcrystalline cellulose triggers ice nucleation in supercooled clouds within the troposphere. The microcrystalline cellulose powder was aerosolized by way of a rotating brush generator and then injected into a ventilated 1.4 m^{-3} chamber vessel. The chamber`s wall temperature was controlled with refrigerated coolant and mechanically evacuating the air all while being simultaneously reducing the thermally insulated vessel. This cooling method allowed for the minimalization of turbulence and temperature fluctuations between the vessel wall and inner gas. The cloud chamber allowed for experiments with water droplet sizes that are relevant to the atmosphere and to control the droplet activation temperature and superstation condition.

Connected to the chamber were a number of particle counters and spectrometers, for example, the condensation particle counter, to monitor the particle size distribution. The aerosol size distributions were measured prior to every ice nucleation experiment, while the optical particle counter was used throughout the entirety of the experiment. This allowed for the parameterization of the ice nucleation

active surface site density (n_s), which represented the ice crystal number concentration in relation to the total surface area concentration of aerosols that had been measured before the start of expansion and adjusted for the pressure dilution that is found within the chamber. There were further studies done on immersion freezing with the two samples using the cold-stage based freezing technique called BINARY. These samples were suspended in bi-distilled water by two different methods, shaken by hand and shaken using a high-speed homogenizer. This method allowed for the ice nucleation active site density per dry mass of cellulose to be determined.

2.6 Arctic – (Irish et al., 2017)

INPs can be found in the sea-surface microlayer and bulk seawater and have been found to affect the freezing capabilities of droplets within mixed phase clouds above -33°C. These particulates can be transferred to the atmosphere through the bubble-bursting mechanism. This sea-surface microlayer is < 1 mm thick and is different from the bulk seawater due to the differences in physical and chemical properties, such as having an enhanced concentration of organic materials.

The ocean has been suggested to be a dominant source of INPs particles within the atmosphere during times when dust concentrations are low. Of the modelling studies, only one has concentrated on the sea-surface microlayer and quantified the INPs. This study added more data to the limited amount on the sea-surface microlayer through the immersion freezing method. The authors investigated the concentrations and properties of the INPs found in the microlayer and bulk seawater samples through the immersion freezing method on samples collected in the Canadian Arctic during the 2014 summer. The arctic was chosen because the clouds in this area are sensitive to atmospheric concentrations and there are no previous studies on the INPs freezing properties from the sea-surface microlayer or bulk

seawater. As the sea ice in the arctic continues to decrease, the sea-surface microlayer and bulk seawater will potentially become more important sources for INPs in that region.

The study chose eight different locations in the Canadian Arctic, and the INPs where found everywhere and were found to freeze at higher temperatures, such as -14°C. These particulates were found in both the sea-surface microlayer and the bulk seawater. The salinity was negated by having a strong negative correlation ($R = 0.7$, $P = 0.02$) after the correction for freezing depression by salts had been applied. One of the possibilities for the INPs being in the bulk seawater could be associated with the melting sea ice. As the ice melts, any particulates that were within the arctic area, or plant substances, would then be in the runoff that ends up in the bulk seawater. The study did find that heating the samples had substantially reduced the INPsactivity, which suggests that heat-labile biological materials were more than likely the source of nucleating activity. The samples were also filtered, which found the particles to be between 0.02 and 0.2 μm. This indicates that the biological materials were more than likely ultramicrobacteria, viruses, or extracellular material. By finding the size, it negated that whole cell bacteria were present within the bulk seawater or within the sea-surface microlayer.

This information was then compared with studies done at other locations and was confirmed to be similar with those study sites. The only major difference between the studies was that, on average, the concentration of INPs were lower than the average found in the other studies, and this anomaly could not be explained with *chlorophyll a* concentrations from the satellite measurements.

2.7 Marine microlayers – (Wilson et al., 2015)

One of the major contributors to atmospheric particles is sea spay, but it is unclear what ice nucleating efficiency it has. The contribution was determined to by the concentration of INPs that were active at -20°C (850 hPa) and compared to the contribution of desert dusts – based on K-feldspar distributions – which indicated that they are competitive with desert sources. These sea-spray particulates have large amounts of organic material that are suspended into the atmosphere through the bubble bursting mechanism that originates at the sea surface microlayer. The organic materials found in the sea surface microlayer make up a substantial fraction of the sea-spray and is 10 ± 5 Tg yr^{-1} of all primary organic aerosols that come from a marine source. There is evidence that proves that cirrus clouds that are over the ocean have interference with ice nucleation from the particles that are emitted by the sea-spray. This study shows the organic material that is found in the sea surface microlayer and its ice nucleation efficiency under conditions relevant in mixed-phase cloud and high-altitude ice cloud formation.

The first step of the experiment was to freeze 1 μL droplets created from microlayer samples collected from the Arctic and Atlantic oceans. They were placed on a cold stage immediately after sampling and cooled until all droplets were frozen. Microlayer droplets were consistently seen to freeze at higher temperatures than the droplets collected from the subsurface water – 2 to 5 m below previous samples at the same location. Using a filtration system, they re-tested the microlayer samples to find that most of the materials that nucleated ice were between 0.2 and 0.02 μm in size. Particles of this size have the potential to be emitted into the atmosphere through the bubble bursting process, which allows the particulates to be a mixture of organics and sea salt.

Another experiment was done on microlayer and surface sea water samples collected from the North Pacific and British Columbia coast by placing them under cirrus cloud conditions. These samples were tested at -40°C and then compared to commercial sea salt and NaCl particles. The surface sea water has a similar activation curve to sea salt and NaCl, and all three showed a sharp increase when the relative humidity was above one hundred and forty three percent with respect to ice. On the other hand, the microlayer had ice formation above the background levels at lower relative humidity in respect to ice. The onset of ice nucleation was seen between one hundred and fifteen percent and one hundred and thirty-three percent relative humidity of ice. The microlayer was efficient deposition mode of ice nucleation particulates, such as Arizona test dust and feldspar at the same particulate size.

To determine if the ice nucleation was caused by inorganics or specific proteins, the microlayer samples were heated up to 100°C and retested because certain proteins that have been identified to be highly active in ice formation denature in heat. By heating the Arctic and Atlantic samples, there was a reduction in ice nucleation activity with a shift towards lower temperatures. The reduction found at three out of four sites implies that there is a presence of thermally liable biological ice nucleation particulates. Through filtration, there were a considerable amount that passed through 0.2 μm filters, which indicates that these particulates are probably smaller biological particulates, such as ultramicrobacteria, viruses, or extracellular material from phytoplankton or bacteria.

CHAPTER III

METHODS

3.1 CRAFT Instruments

National Institute of Polar Research and West Texas A&M University both house a CRAFT. The CRAFT is a cold-stage freezing technique that allows immersing particulates within droplets and monitoring the droplet freezing as a function of temperatures that are relevant within mixed-phase clouds (Tobo, 2016). There were a set of uncertainties with both the NiPR-CRAFT and the WT-CRAFT. On a bulk sample run on the NiPR-CRAFT, there was a variance of ± 0.2°C; also, the WT-CRAFT had a 23.5% uncertainty based on the standard error of three samples with a temperature variance of ± 0.5°C (Hiranuma et al., 2018, ACPD).

The National Institute of Polar Research's Cryogenic Refrigerator Applied Freezing Test (NiPR-CRAFT; Tobo, 2016) is held within a clean booth with two filters pulling air out of the area. One filter is placed at the top of the clean booth pulling the air out of the booth, and the other is placed in a prep area pulling air away from the droplets. Figure 3.1 shows the general schematic of CRAFT. There is a video camera placed above the Cryo Porter, which is a cooling cell, to record the droplets freezing. With the NiPR-CRAFT, the droplets have a volume of 5 µL with forty-nine droplets in total. Droplets are placed on an aluminum plate with a layer of Vaseline (with no additives) to create a hydrophobic layer and to prevent contact freezing. The samples are then monitored as the NiPR-CRAFT is reduced from -5℃ to -40℃ at 1℃ per minute. The freezing rate is calculated every half a degree by

manually counting how many droplets are frozen relative to a total number of droplets.

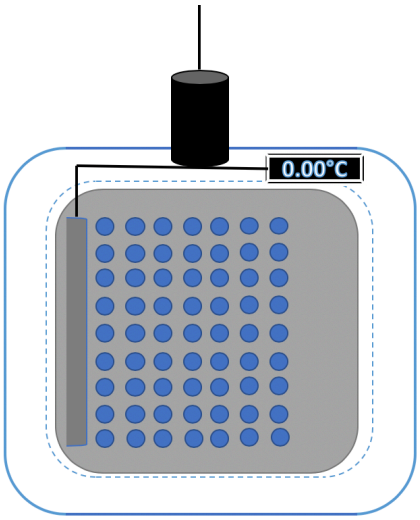

Fig. 3.1: General schematic overview of the CRAFT.

West Texas A&M University's Cryogenic Refrigerator Applied Freezing Test (WT-CRAFT) is placed within a chemical fume hood, which contains the air and ventilates it out of the area from the bottom to the top of the fume hood (Hiranuma et al., 2018). Like the clean booth, the plating of the droplets is done within the fume hood. The droplets used in the WT-CRAFT were reduced to 3 µL with seventy in total. This decrease in droplet size was compared to what is employed in NiPR-CRAFT (5 µL) to reduce the number of particulates exposed to the ambient air and could minimize the number of artifacts. Droplets are placed on an aluminum plate with a layer of Vaseline (with no additives) to create a hydrophobic layer that prevents contact freezing from occurring. The WT-CRAFT has a video camera placed above to Cryo Porter to monitor the droplets freezing from -5°C to -40°C at a rate of 1°C per minute. Every half a degree, the freezing rate is observed by comparing the unfrozen to the total number of droplets.

3.2 Ice Nucleation Parameterizations

Ice nucleation parameterizations employed in this study were based off of two previous studies. For the cellulose study, I followed the Tobo 2016 (T16) parameterization for immersion freezing (Tobo, 2016). The arctic studies parameters were based off of the DeMott 2017 parameterization (D17) on comparing ambient atmospheric concentration measurements (DeMott et al., 2017). The following equation was used to calculate the number of active sites per unit of water (L^{-1}) at any temperature (T);

$$K\ (T) = -\ ln\frac{(1-f_{\text{frozen}}(T))}{V_{\text{drop}}} = -ln\frac{(f_{\text{unfrozen}}(T))}{V_{\text{drop}}} \qquad \text{Eqn. (1)}$$

where V_{drop} is the volume of the droplet, f_{frozen} is the number of frozen droplets at the specified temperature, and the reverse for $f_{unfrozen}$. The second equation below was used to determine the active site density per unit mass ($n_m(T)$, g^{-1});

$$n_m(T) = K(T) \cdot \frac{d}{C_m} \qquad \text{Eqn. (2)}$$

in which, C_m being the mass concentration of the particles in the solution and d being the dilution ratio. Next, the equation (3) was used to determine the active site density per unit surface area (n_s (T), m^{-2});

$$n_s(T) = n_m(T) \cdot \left[\frac{S_{Total}}{M_{Total}}\right]^{-1} \qquad \text{Eqn. (3)}$$

where S_{Total} is the surface and M_{Total} is the mass and together make the surface-to-mass ration. Finally, the equation (4) was used to determine the number of INPs per unit volume of air;

$$n_{INPs}(T) = K(T)\left(\frac{V_w}{V_s}\right) \qquad \text{Eqn. (4)}$$

where V_w is the volume of liquid and V_s is the sampled volume of air (L).

As the n_m lines appear straight, the data were patched together with the dilutions in mind. Al the replicated samples were put side by side at each dilution to

determine the start temperature and to look for the overlap of dilutions. At that point, the replications are averaged out and patched together into a single line. In Appendix A, there is a table containing all acronyms and units used within the paper.

3.3 Water Background

In this study, all samples were suspended in water to create a suspension sample. Prior to running any of the samples, two different types of water were tested on the WT-CRAFT at different volumes to determine what background interferences would be coming from the solvent in the solution. The two types of water tested were deionized water and Milli-Q water, and the volumes tested were 1 µL, 3 µL, and 5 µL (**Fig. 3.2**). For each water type, there was notable variance in freezing capability based on volume. As for the deionized water, the onset freezing capability was 10°C higher than the Milli-Q water presumably due to the introduction of artifacts acting as INPs. Due to fewer artifacts within the water, Milli-Q water was used in this study.

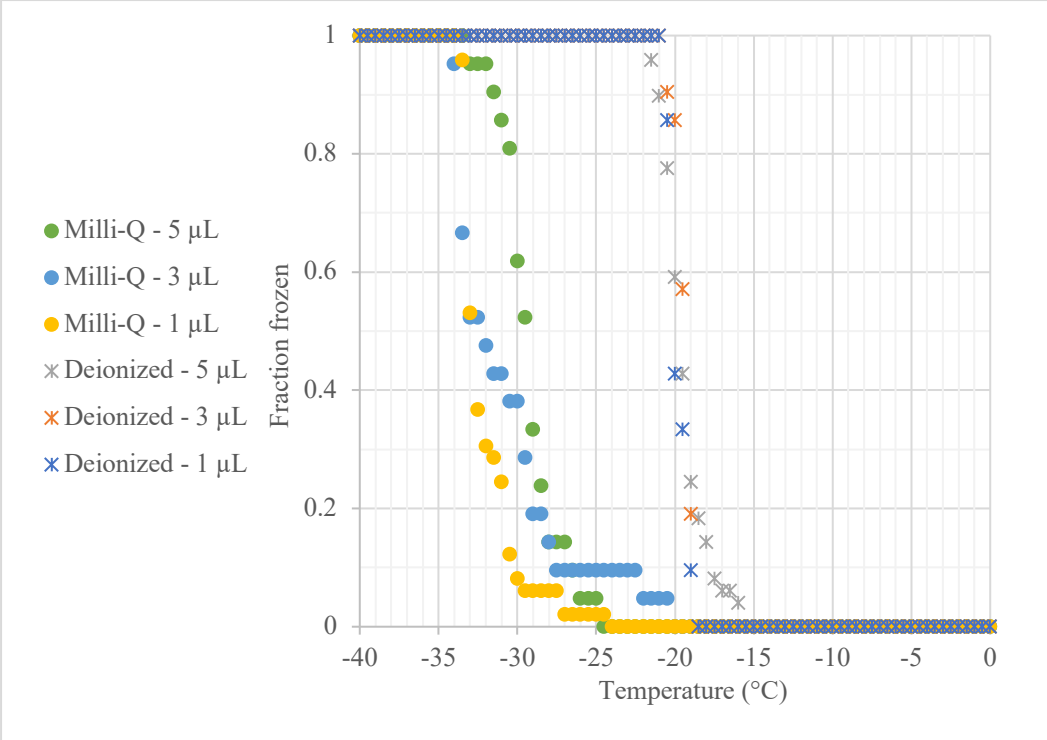

Fig. 3.2: Water freezing spectra of Milli-Q and Deionized water

3.4 Cellulose Sample

The laboratory cellulose used in the study were pre-prepared, available to purchase off the shelf, in varying methods. Starting with the Nanocrystalline, TEMPO-CNF was created in Dr. Isogai's research lab by oxidizing the C6 primary hydroxyl group within a wood cellulose to carboxylate group a TEMPO catalyst, which are then followed with successive mechanical treatments (Isogai et al., 2011). For the difference between the standard (3 nm) and the short (< 3 nm), the mechanical treatments were used longer to continue the isolation of fibers. Next, the CM-CNF sample was created by arbitrary carboxymethylation – a process of negatively charging the surface to promote stability from the carboxymethylated fibers and break up the lulosic fibers – of the primary and secondary hydroxyl groups of C2, C3, and C6 which were then put through successive mechanical fibrillation – isolation of cellulose fibers through hydrodynamic forces causing high intensive waves (manufacturer report; Abdul Khalil et al., 2014). The powder form was collected prior to mechanical fibrillation previously described, where the gel form went through multiple rounds of said fibrillation. Lastly, NCC is created through the extraction from the sludge produced by the paper industry. To do this, the Melodea group takes the cellulose fibers that contain amorphous and crystalline areas and use an acid hydrolysis to create high-purity singular crystals within the suspension (Melodea Bio Based Solutions). The NCC is then recovered with repeated water bath cycles, and then they sonicate the solution to break the structures apart into a stable suspension (Melodea Bio Based Solutions).

The first Microcrystalline cellulose is MCC, which was recovered from amorphous regions that were hydrolyzed, leaving behind crystalline microfibrils (manufacturer report). Sigma-Adlrich extracted FC from natural wood pulp

(Hiranuma et al., 2015). For the next microcrystalline cellulose, α-cellulose is a polysaccharide that is composed of long chains consisting of β(1,4) and is linked with D-glucose units (Manufacturer report). Lastly, Arbo cellulose is created from organic fibers that were obtained through the chemical disintegration of fir and beech woods (ARASH AZMA 2).

Table 3.1: All microcrystalline and nanocrystalline cellulose samples used within the study.

Cellulose Type	Samples	Product Form	Manufacturer-reported Diameter	Droplet Size Examined in this Study	wt% Examined in this Study
Nano-crystalline	**TEMPO-CNF Short (Nippon Paper industries)**	Gel	<3 nm	5 µL/3 µL	0.1-0.00001
	TEMPO-CNF standard (Nippon Paper industries)	Gel	3 nm	5 µL/3 µL	0.1-0.00001
	CM-CMF (Nippon Paper Industries)	Powder	3-15 nm	5 µL/3 µL	0.1-0.000001
	CM-CMF (Nippon Paper Industries)	Gel	3-15 nm	5 µL/3 µL	0.1-0.000001
	NCC (Melodea, WS1)	Powder	5-20 nm width, 100-500 nm length	5 µL	0.1-0.00001
Micro-crystalline	**MCC (Aldrich, 435236)**	Powder	51 µm	5 µL/3 µL	0.05-0.0005
	FC (Sigma, C6288)	Powder	N/A	5 µL/3 µL	0.05-0.0005
	α-cellulose (Sigma, C8002)	Powder	N/A	3 µL	0.05-0.0005
	Arbo-cellulose (JRS Rettenmaier & Söhne, ARBOCZL)	Powder	18-35 µm	3 µL	0.05-0.0005

3.5 The Arctic Filter Samples

In Ny-Ålesund, Svalbard (**Fig. 3.3**), ten samples were collected on 47 mm Nucleopore membrane filters at the Gruvebadet observatory, which is about 55 m above sea level. The schematic of the sampling system is shown in Figure 3.4 in which the samples were collected through during the period of March 2-27 of 2017. This system allows air to enter the TSP inlet and pass through the nucleopore filter.

With one exception, the samples were collected at the observatory; this exceptional sample was collected at the Amundsen-Nobile Climate Change tower located in close proximity to the observatory. This location is also about 55 m above sea level. The TSI4100 flow meter allowed for the volume of air to be monitored as the air passes through, and the total volume of air passed through the cross section of filter to determine the specific water volume required for target weight percent, as shown in Table 3.2.

Table 3.2: All arctic samples that were collected from Ny-Ålesund, Svalbard.

Experimental #	Date of collection	Total Vol. of air (L) for 50% cross section of filter sampling	Vol.of H2O (L) for suspension generation [wt%]
A-CARE_GB_01	20170302-20170303	5.43×10^3	1.32 [1.1×10^{-4} – 1.1×10^{-7}]
A-CARE_GB_02	20170303-20170305	9.39×10^3	1.14 [1.59×10^{-3} – 1.59×10^{-6}]
A-CARE_GB_03	20170305-20170307	9.02×10^3	1.1 [2.12×10^{-3} – 2.12×10^{-6}]
A-CARE_GB_04	20170308-20170310	1.03×10^4	1.25 [1.86×10^{-3} – 1.86×10^{-6}]
A-CARE_GB_05	20170310-20170312	9.25×10^3	1.12 [3.78×10^{-3} – 3.78×10^{-6}]
A-CARE_GB_06	20170312-20170314	9.12×10^3	1.11 [1.39×10^{-3} – 1.39×10^{-6}]
A-CARE_ANCCT_07	20170316-20170321	2.64×10^4	3.2 [1.97×10^{-3}– 1.97×10^{-6}]
A-CARE_GB_08	20170322-20170324	1.09×10^4	1.33 [1.39×10^{-3} – 1.39×10^{-6}]
A-CARE_GB_09	20170325-20170327	9.16×10^3	1.11 [2.38×10^{-3} – 2.38×10^{-6}]
A-CARE_GB_10	20170327-20170330	1.33×10^4	1.62 [2.3×10^{-3}– 2.3×10^{-6}]

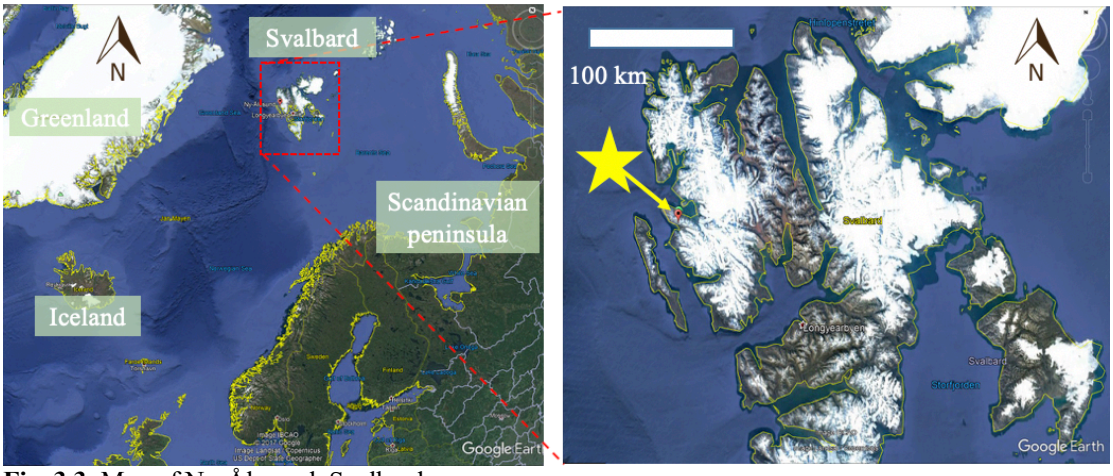

Fig. 3.3: Map of Ny-Ålesund, Svalbard.

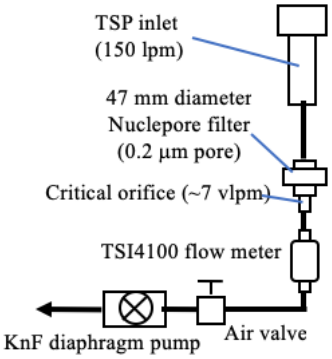

Fig. 3.4: Schematics of the sampling system.

3.6 Cellulose Analysis

Water suspended samples were created based on a weight percent. All nanocrystalline cellulose have a 0.1 wt % and all microcrystalline cellulose have a 0.05 wt %. All samples were originally created at 0.1 or 0.05 wt % for the initial suspension due to it being the upper limit for minimum sedimentation (Hiranuma et al., 2018, ACPD). To create the initial stock solutions, cellulose powders/gels were weighed using a microbalance (OHAUS balance, Adventurer) and a flat-bottomed tube or weigh boat. Then, a known amount of weighted powders/gels were suspended into Milli-Q water (resistivity of 18.2 MΩ cm^{-1} at 25°C). Nanocrystalline cellulose suspensions were placed on a vibrating machine to pulverize/deagglomerate the particulates throughout the water – Tables 3.3 and 3.4 summarize both samples created at West Texas A&M University and National Institute of Polar Research. Microcrystalline cellulose samples were sonicated for fifteen minutes and let to settle for 30 minutes prior to CRAFT experimentation – Table 3.5 shows all samples that were conducted with a brief description of how the sample was created and by whom. This is to allow the larger particulates to settle to the bottom and allow for the experiment to be run on the particulates that could potentially be found in the atmosphere. Samples are then diluted by tenfold until I observed one hundred percent Frozen Fraction at -30°C, or lower temperatures. A serial dilution was carried out

based on a constant step dilution with no varying amounts that is typically used in a Microbiological setting (Bauman, 2017). More specifically, Figure 3.5 shows the ten- and hundred-fold step dilution that was used within these experiments. The ten-fold dilution was created by taking 0.120 mL of the stock solution and adding it to 1.08 mL of Milli-Q; while the hundred-fold was created by taking 0.040 mL of the stock solution into 3.96 mL of Milli-Q. These small amounts allowed for a standardized formation of dilution when there is a chance for having less than 1 mL in the stock solution.

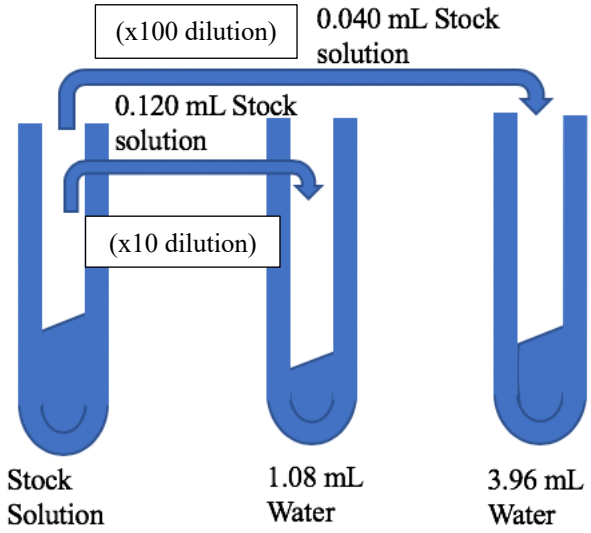

Figure 3.5: Dilution map for all samples starting with the original stock solution.

Table 3.3: All nanocrystalline experiments conducted at West Texas A&M University with the number of experiments per solution, the dilution factor, a small note of how it was created, who conducted the experiment, and the quantity and volume of droplets.

West Texas A&M University - Nanocrystalline Cellulose			
Sample/wt%	**0.1**	**0.01**	**0.001**
CM-CNF powder	1 - 10min vibration (JM - 3uLx70d)	1 - 30s handshaken (JM - 3uLx70d)	1 - 30s handshaken (JM - 3uLx70d)
CM-CNF gel	1 - 10min vibrated (ZS - 3uLx70d) 1 - rerun (KC - 3uLx70d) 1 - 10min vibration (KC - 3uLx70d) 1 - 10min vibration (KC - 3uLx70d) 1 - 10min vibration (KC - 3uLx70d)	1 - 30s handshaken (KC - 3uLx70d) 1 - 30s handshaken (KC - 3uLx70d)	1 - 30s handshaken (KC - 3uLx70d) 1 - 30s handshaken (KC - 3uLx70d)
TEMPO-CNF short	1 - 10min vibration (KC - 3uLx70d)	1 - 30s handshaken (KC - 3uLx70d)	1 - 30s handshaken (KC - 3uLx70d)
TEMPO-CNF standard	1 - 10min vibration (KC - 3uLx70d)	1 - 30s handshaken. (KC - 3uLx70d)	1 - 30s handshaken (KC - 3uLx70d) 1 - 30s handshaken (KC - 3uLx70d)
Sample/wt%	**0.0001**	**0.00001**	
CM-CNF powder	2 - 30s handshaken. (JM - 3uLx69d(1)70d(2))	1 - 30s handshaken (JM - 3uLx70d)	

CM-CNF gel	1 - 30s handshaken (KC - 3uL7x70d)	-
TEMPO-CNF short	-	-
TEMPO-CNF standard	-	-

Table 3.4: All nanocrystalline experiments conducted at National Institute of Polar Research with the number of experiments per solution, the dilution factor, a small note of how it was created, who conducted the experiment, and the quantity and volume of droplets.

National Institute of Polar Research - Nanocrystalline Cellulose			
Sample/wt%	**0.1**	**0.01**	**0.001**
CM-CNF powder	3 - 10min vibration (KC - 5uLx49d) 1 - 10min vibration (KC - 5uLx49d)	3 - 30s handshaken (KC - 5uLx49d) 1 - 30s handshaken (KC - 5uLx49d)	4 - 30s handshaken (KC - 5uLx49d) 1 - 30s handshaken (KC - 5uLx49d)
CM-CNF gel	1 - 10min vibration (KC - 5uLx49d) 3 - 10min vibration (KC - 5uLx49d)	1 - 30s handshaken (KC - 5uLx49d) 2 - 30s handshaken (KC - 5uLx47d(1)49d(2))	1 - 30s handshaken (KC - 5uLx49d) 1 - 30s handshaken (KC - 5uLx49d)
TEMPO-CNF short	1 - 10min vibration (KC - 5uLx49d) 1 - 10min vibration (KC - 5uLx49d)	1 - 30s handshaken (KC - 5uLx50d) 1 - 30s handshaken (KC - 5uLx49d)	1 - 30s handshaken (KC - 5uLx49d) 1 - 30s handshaken (KC - 5uLx49d) 1 - 30s handshaken (KC - 5uLx49d)
TEMPO-CNF standard	1 - 10min vibration (KC - 5uLx49d) 1 - 10min vibration (KC - 5uLx49d) 1 - 10min vibration (KC - 5uLx49d)	1 - 30s handshaken (KC - 5uLx49d) 2 - 30s handshaken (KC - 5uLx49d) 1 - 30s handshaken (KC - 5uLx49d)	1 - 30s handshaken (KC - 5uLx49d) 1 - 30s handshaken (KC - 5uLx49d)
NCC	1 - 10min vibration (KC - 3uLx64d) 1 - 10min vibration (KC - 5uLx49d)	1 - 30s handshaken (KC - 5uLx50d)	1 - 30s handshaken (KC - 5uLx49d)
Sample/wt%	**0.0001**	**0.00001**	**0.000001**
CM-CNF powder	4 - 30s handshaken (KC - 5uLx49d) 4 - 30s handshaken (KC - 5uLx49d(1,2,4)41d(3))	-	-
CM-CNF gel	1 - 30s handshaken (KC - 5uLx49d) 1 - 30s handshaken (KC - 5uLx49d)	1 - 30s handshaken (KC - 5uLx49d) 1 - 30s handshaken (KC - 5uLx49d)	1 - 30s handshaken (KC - 5uLx49d) 1 - 30s handshaken (KC - 5uLx49d)
TEMPO-CNF short	1 - 30s handshaken (KC - 5uLx49d) 1 - 30s handshaken (KC - 5uLx49d) 1 - 30s handshaken (KC - 5uLx49d)	1 - 30s handshaken (KC - 5uLx49d) 3 - 30s handshaken (KC - 5uLx49d) 2 - 30s handshaken (KC - 5uLx49d) 1 - 30s handshaken (KM - 5uLx49d) 1 - 30s handshaken (KC - 5uLx49d)	-
TEMPO-CNF standard	1 - 30s handshaken (KC - 5uLx49d) 2 - 30s handshaken (KC - 5uLx49d)	-	-
NCC	1 - 30s handshaken (KC - 5uLx49d)	2 - 30s handshaken. (KC - 5uLx49d)	-

Table 3.5: All microcrystalline experiments conducted at West Texas A&M University with the number of experiments per solution, the dilution factor, a small note of how it was created, who conducted the experiment, and the quantity and volume of droplets.

West Texas A&M - Microcrystalline Cellulose		
Sample/wt%	**0.05**	**0.005**
FC	1 - 15min sonication/shaken every 2 rows (CW - 5uLx49d) 1 - 30s handshaken (CW - 5uLx49d) 1 - 30s handshaken (KC - 5uLx49d) 1 - 15min sonication/shaken every 2 rows (KC - 5uLx49d) 1 - 15min sonication/shaken every 2 rows (CW - 5uLx49d) 1 - 30s handshaken (CW - 3uLx49d) 1 - 15min sonication/shaken every 2 rows (CW - 3uLx49) 1 - 30s handshaken (CW - 3uLx49d) 1 - 15min sonication/shaken every 2 rows (KC - 3uLx49d) 1 - 15min sonication/shaken every 2 rows (CW - 3uLx49d)	1 - 15min sonication/shaken every 2 rows (KC - 5uLx49d) 1 - 30s handshaken (KC - 5uLx49d) 1 - 15min sonication/shaken every 2 rows (KC - 3uLx49d) 1 - 30s handshaken (KC - 3uLx49d) 1 - 15min sonication/shaken every 2 rows (CW - 3uLx49d) 2 - 30s handshaken (CW - 3uLx49d) 1 - 30s handshaken (KC - 3uLx49d)
MCC	1 - 15min sonication/shaken every 2 rows (CW - 5uLx49d) 1 - 30s handshaken (CW - 5uLx49d) 1 - 15min sonication/shaken every 2 rows (CW - 5uLx49d) 1 - 30s handshaken (CW - 5uLx49d) 1 - 30s handshaken (KC - 5uLx49d) 1 - 15min sonication/shaken every 2 rows (KC - 5uLx49d) 1 - 15min sonication/shaken every 2 rows (CW - 5uLx49d) 1 - 30s handshaken (CW - 3uLx49d) 1 - 15min sonication/shaken every 2 rows (CW - 3uLx49d) 1 - 30s handshaken (CW - 3uLx49d)	1 - 15min sonication/shaken every 2 rows (CW - 5uLx49d) 1 - 30s handshaken (CW - 5uLx49d) 1 - 30s handshaken (KC - 5uLx49d). 1 - 15min sonication/shaken every 2 rows (CW - 5uLx49d) 1 - 15min sonication/shaken every 2 rows (KC - 5uLx49d) 2 - 15min sonication/shaken every 2 rows (CW - 3uLx49d) 2 - 30s handshaken (CW - 3uLx49d)
Arbo-cellulose	1 - 10min handshaken (KC - 3uLx70d) 1 - 15min sonication/shaken every 2 rows (KC - 3uLx49d)	1 - 30s handshaken (KC - 3uLx70d) 1 - 30s handshaken (KC - 3uLx49d)
α-cellulose	1 - 10min handshaken (KC - 3uLx67d) 1 - 10min handshaken (KC - 3uLx70d) 1 - 10min vibration (KC - 3uLx69d) 1 - 2wk handshaken time trial (KC - 3uLx70d) 1 - 1wk vibration time trial (KC - 3uLx69d) 1 - 15min sonication/30min set (KC - 3uLx70d) 1 - 15min sonication/shaken every 2 rows (KC - 3uLx49d)	1 - 30s handshaken (KC - 3uLx70d) 1 - 30s handshaken (KC - 3uLx70d) 1 - 30s handshaken (KC - 3uLx70d) 1 - 2wk handshaken time trial (KC - 3uLx70d) 1 - 1wk vibration time trial. (KC - 3uLx70d) 2 - 30s handshaken/10min set (KC - 3uLx70d) 1 - 30s handshaken/10min set (KC - 3uLx70d) 1 - 30s handshake (KC - 3uLx49d)
Sample/wt%	**0.0005**	
FC	1 - 15min sonication/shaken every 2 rows (CW - 3uLx49d) 1 - 15min sonication/shaken every 2 rows (CW - 3uLx49d) 1 - 30s handshaken (CW - 3uLx49d) 1 - 30s handshaken (CW - 3uLx49d)	
MCC	1 - 15min sonication/shaken every 2 rows (CW - 3uLx49d) 1 - 30s handshaken (CW - 3uLx49d)	
Arbo-cellulose	1 - 30s handshaken (KC - 3uLx69d) 1 - 30s handshaken (KC - 3uLx49d)	
α-cellulose	1 - 30s handshaken (KC - 3uLx70d) 1 - 30s handshaken (KC - 3uLx70d)	

3.7 Arctic Analysis

These Nucleopore filter suspensions were prepared in a sterile booth to prevent any additional particulates from being introduced. To prevent that, the area is stylized with 70% isopropyl alcohol and had a protective layer of aluminum foil and sterile petri dishes. Only fifty percent of the filter was used to allow for the other half to be used in a replication study. To retrieve the half used in the study, all utensils were sterilized by the same method and the tweezers were only used on the outermost edge where a ring was placed during collection. The filter is then cut into four and placed in a falcon tube with Milli-Q water (at the least limiter) to create a weight percent based on the known weight of the particulates. By using the least limiter, the concentration is closer to replicating what is occurring within the droplets within the atmosphere. The filter is cut into four to submerge as much of it into the water and remove as many particulates as possible. Samples are then hand shaken for ten minutes rather than vibrated to prevent the breakdown of the filter into the solution. Once the first solution for the sample is created, the dilutions are created following the same method, as described in section 3.6 (**Fig. 3.5**). These samples were only diluted down to a hundred-fold because after would fall back into the water line indicating no particles of consequence involved (**Fig. 3.6)**. After the samples were run, they were stored at 4°C with the lid wrapped in parafilm to prevent any introduction of new particles.

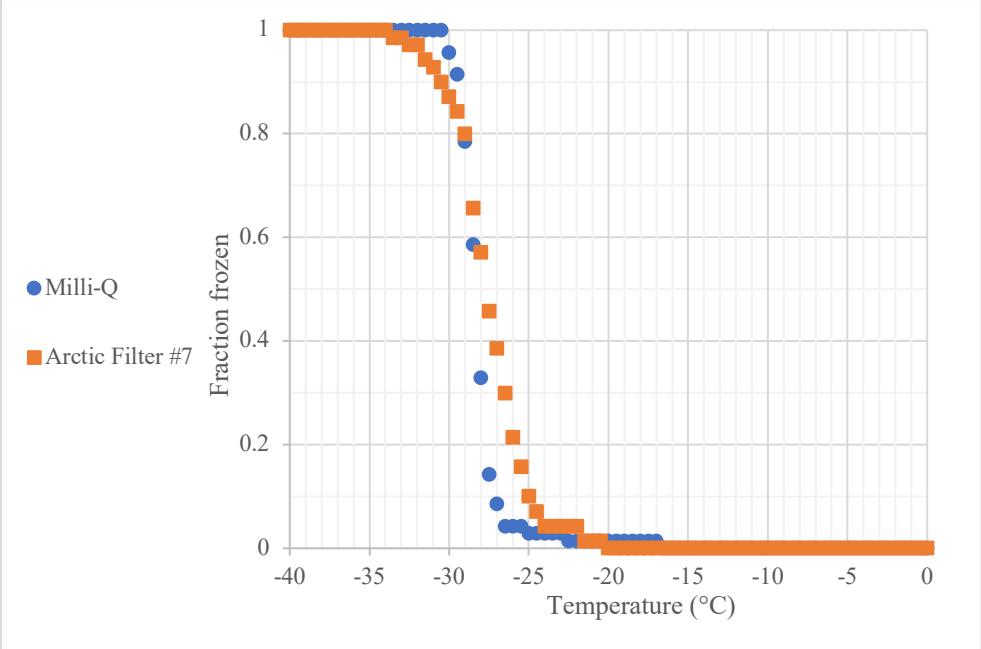

Fig. 3.6: Background comparison of Milli-Q and dilution of sample until the water line and droplet line overlap each other.

CHAPTER IV

CELLULOSE RESULTS

4.1 Frozen Fraction

The Frozen fraction is the number of frozen droplets compared to the total number of droplets examined at every half a degree from 0°C to -40°C. For the original stock solution with a 0.1 wt % in Figure 4.1, three of nanocrystalline samples (CM-CNF gel, TEMPO-CNF short, and TEMPO-standard) have a similar freezing efficiency within a temperature range from -11°C to -17°C. All other 0.1 wt % samples froze at the temperatures from -17°C to -23°C. The powder CM-CNF that has been run at both institutes had a half a degree difference at ~74 (WT-CRAFT) and 79 (NiPR-CRAFT) percent of the droplets frozen at -21°C to -21.5°C, respectively shown in Figure 4.2. More detailed discussion is followed in Section 4.6. By only showing the original stock solution of 0.1 wt %, the initial reaction of the suspensions is comparable.

As shown in Figure 4.3, all 0.05 wt % microcrystalline cellulose suspensions froze within the temperature range of -14°C and -23°C. The sample FC had a higher freezing efficiency than all other microcrystalline samples by freezing 0.5-1° earlier than the others. Microcrystalline cellulose had lower freezing efficiency than three of the nanocrystalline cellulose (CM-CNF gel, TEMPO-CNF short, and TEMPO-standard). As for the other two nanocrystalline cellulose samples, they had a similar freezing temperature range as the microcrystalline.

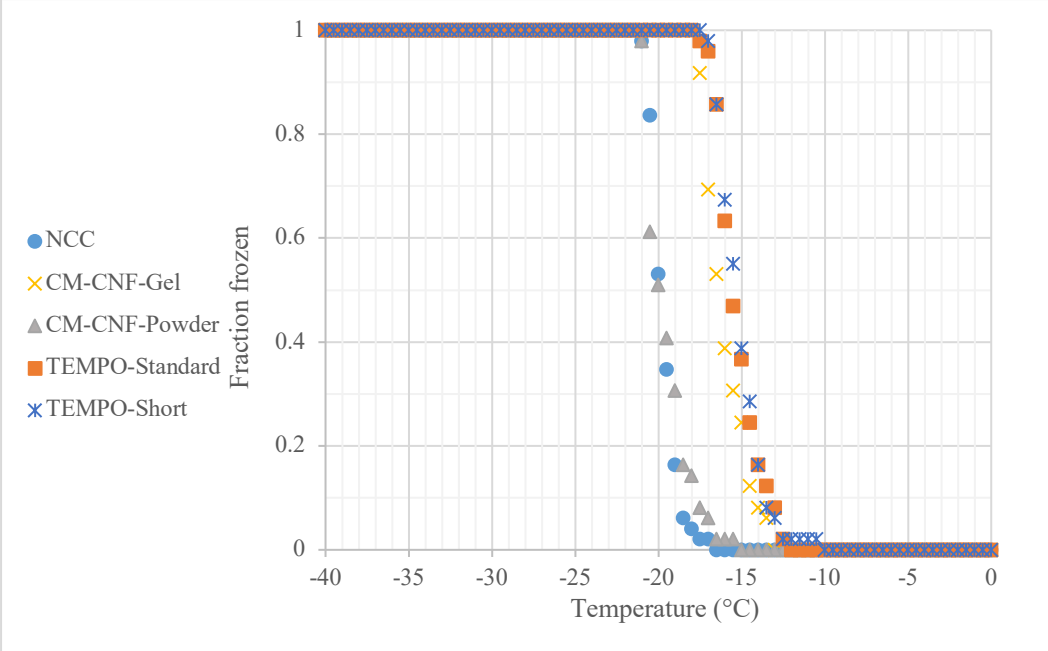

Fig. 4.1: Frozen Fraction of nanocrystalline cellulose based solely on the stock solution at 0.1 wt %.

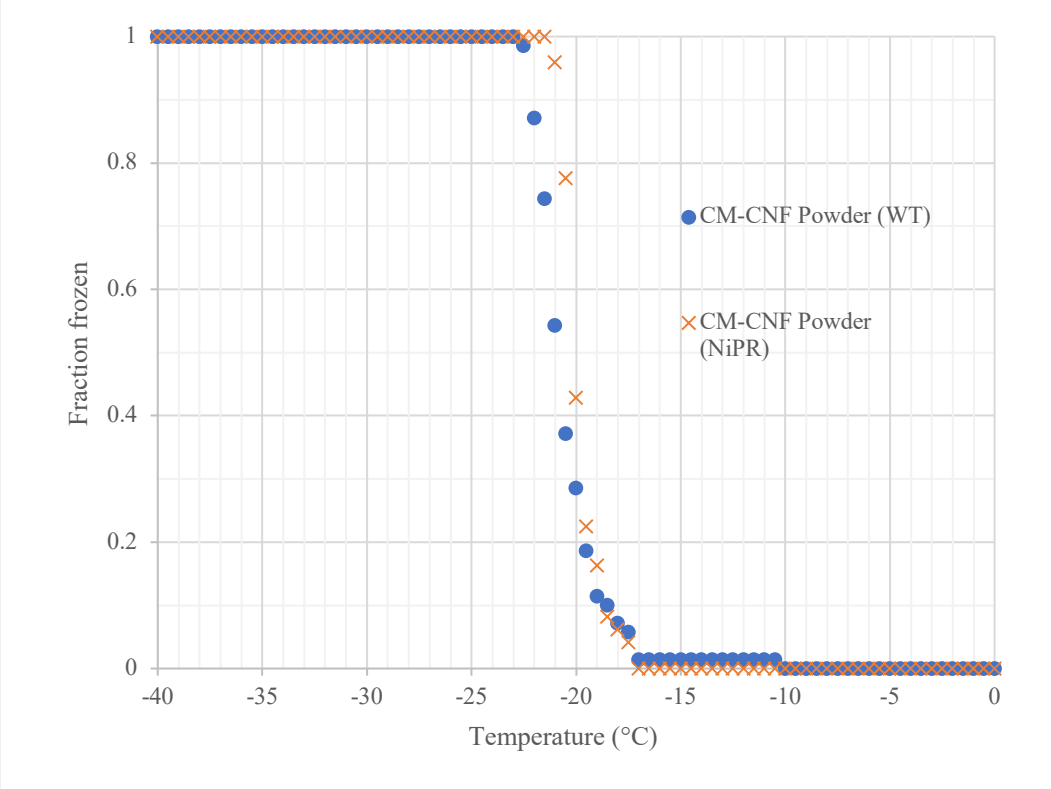

Fig 4.2: Frozen Fraction comparison of CM-CNF Powder between WT and NiPR.

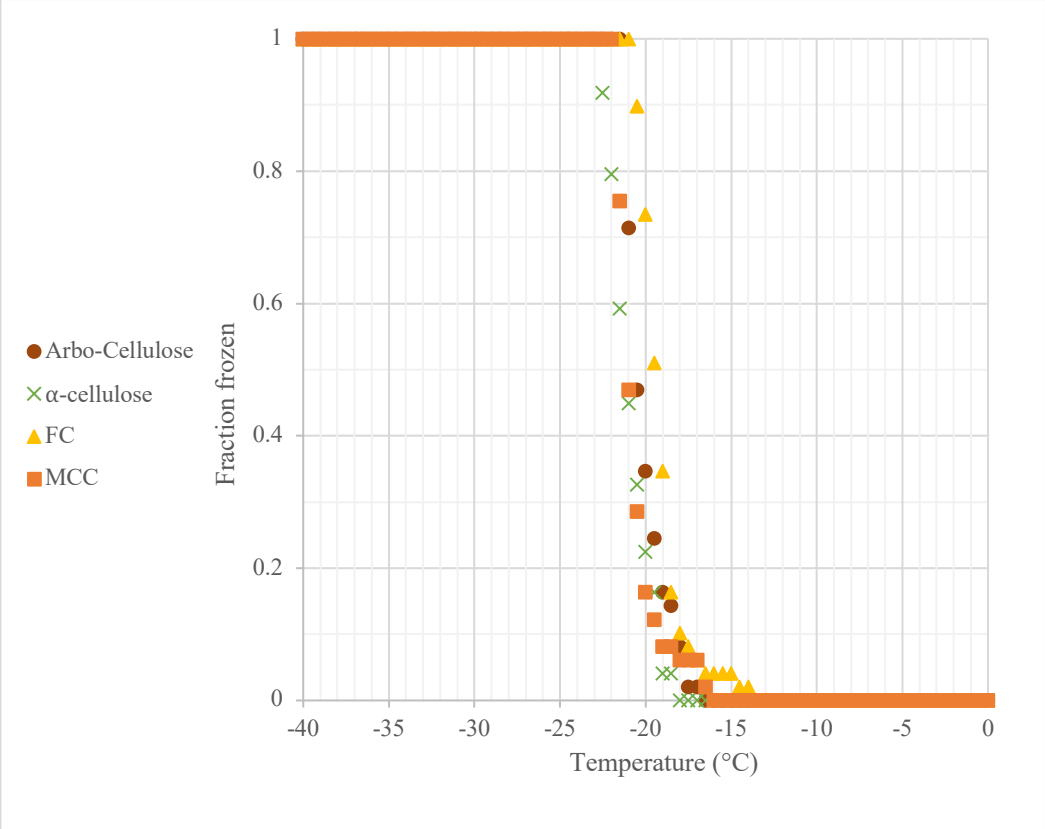

Fig. 4.3: Frozen Fraction of microcrystalline cellulose based solely on the stock solution at 0.05 wt %.

All samples were diluted until they folded back into the water. The dilutions could range anywhere from 0.01 to 0.00001 wt %. In Figure 4.4, the α-cellulose sample has been diluted to 0.0005 wt % compared to the Milli-Q used to create the suspension. Once any of the results have folded back into the water line, the dilution sample is then omitted due to insufficient particulates within the solution.

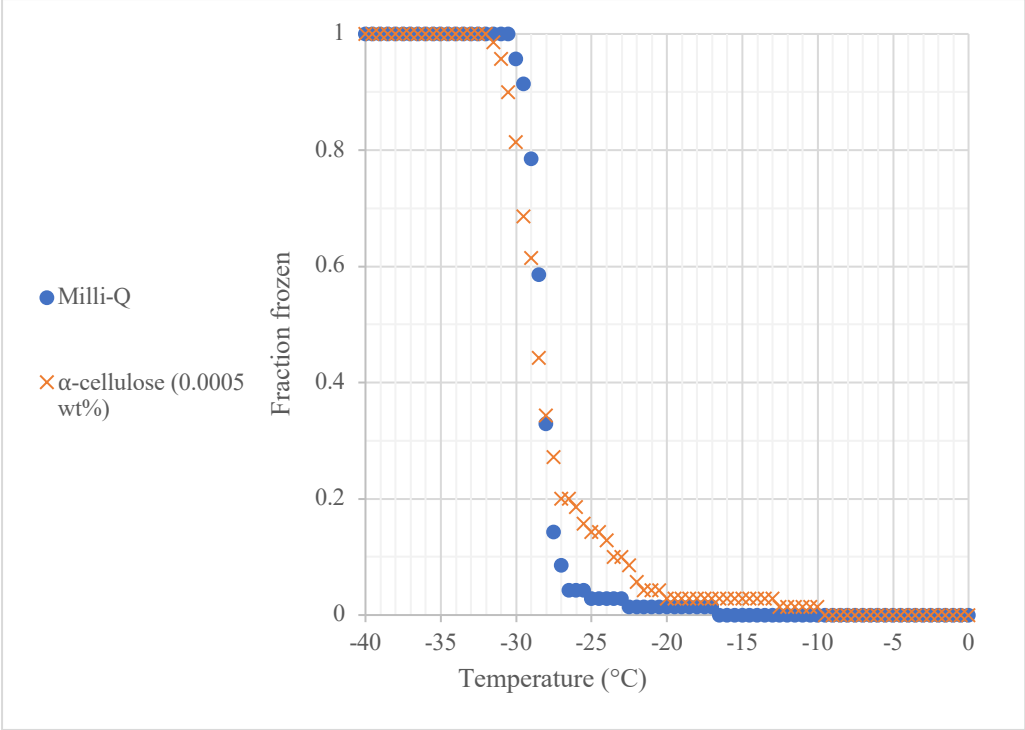

Fig 4.4: Background comparison of Milli-Q and dilution of sample until omission.

4.2 n_m

Figure 4.5 shows that NCC and powder CM-CNF have similar n_m curves with NCC being a half an order of magnitude more active. The short and standard length of TEMPO-CNF have half an order of magnitude difference at -30°C with TEMPO-CNF short having more active mass density per unit than the standard form. As for CM-CNF, the powder and gel have a difference of one and a half orders of magnitude at -30°C with the gel form being more active. Possible reasons for this occurrence are discussed in Chapter 6.1 Cellulose.

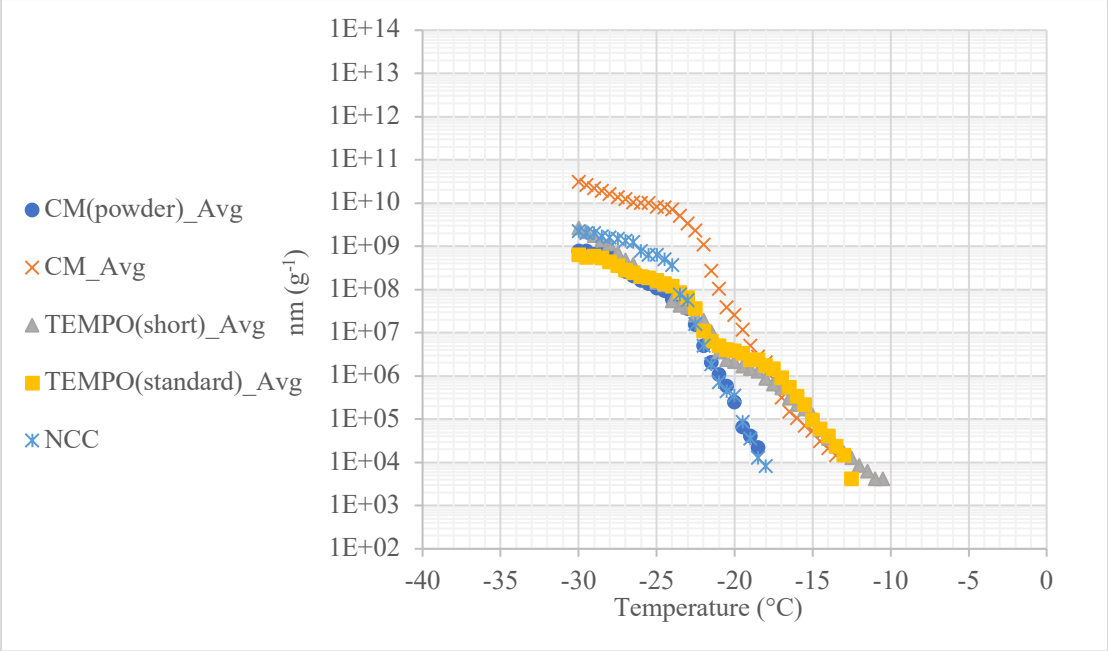

Fig. 4.5: The active site density per unit of mass of nanocrystalline cellulose.

Within the microcrystalline cellulose (**Fig. 4.6**), the samples started with similar n_m with 1E+04 g^{-1}. As the temperature reaches -20°C, FC and Arbo-cellulose were half an order of magnitude more active than MCC and α-cellulose. The separation of samples was more distinct in the microcrystalline cellulose than in the nanocrystalline cellulose. MCC and α-cellulose have similar n_m curves until the end where α-cellulose finished at -27°C and MCC finished at -30°C. Initially at higher temperatures, TEMPO-CNF short, TEMPO-CNF standard, and CM-CNF gel are similar in the initial ice nucleation activation. CM-CNF powder and NCC had an initial activation at lower temperature – ~6° lower – as compared to the other three samples. At lower temperatures (-25°C to -30°C), CM-CNF powder and TEMPO-CNF short were similar activation sites with 1E+09.2 g^{-1}, while TEMPO-CNF standard and CM-CNF powder had 1E+09 g^{-1} activations sites. This shows that, initially, TEMPO-CNF standard initially had similar activation as CM-CNF gel at higher temperatures and CM-CNF powder at lower temperatures. A more detailed discussion of what causes these discrepancies is given in Chapter 6.1 Cellulose.

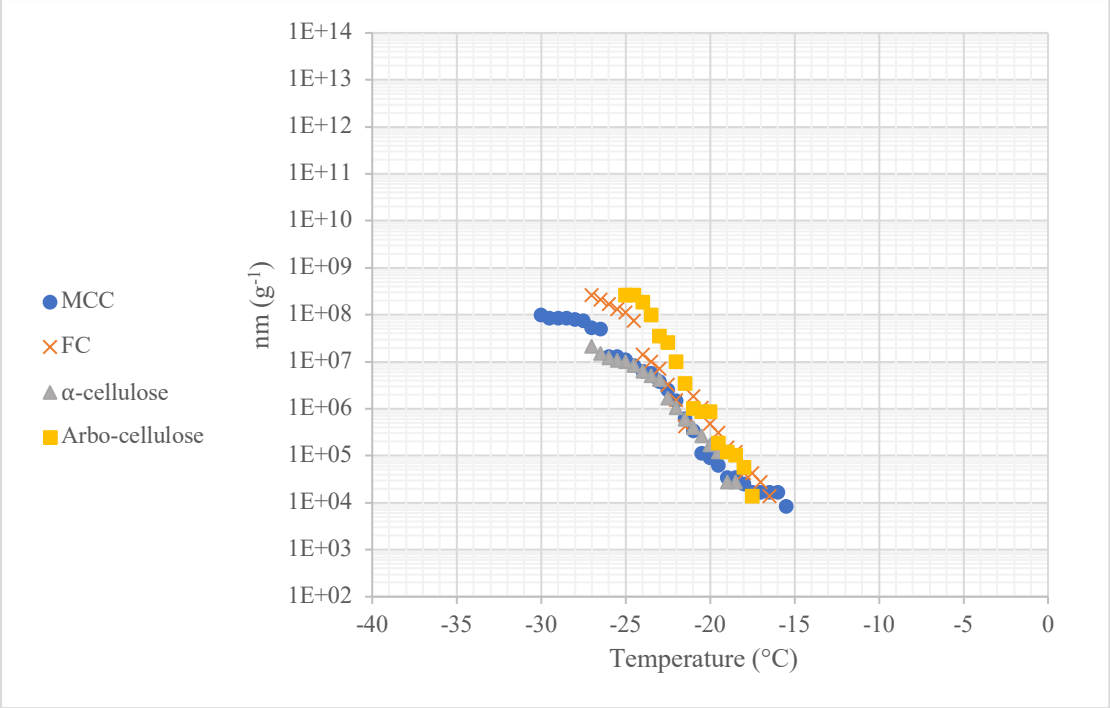

Fig. 4.6: The active site density per unit of mass of microcrystalline cellulose.

4.3 α-cellulose and FC Time trial

A time trial was done on α-cellulose to look at degradation over time (**Fig. 4.7)**. One sample (**a**) was vibrated for ten minutes while the other (**b**) was hand shaken for ten minutes. The vibrated sample was experimented on the day of creation and a week later. As for the hand shaken sample, it was experimented on the day of creation and two weeks later. There was no difference in ice nucleation efficiency between sonication and hand shaken, nor any indication of degradation of the 0.05 wt % solutions over the one- or two-week time. This indicated that regardless of sample preparation of vibrating or handshaking for ten minutes and did not have any variance between the ice nucleation efficiency and no decay of freezing capability over the given time.

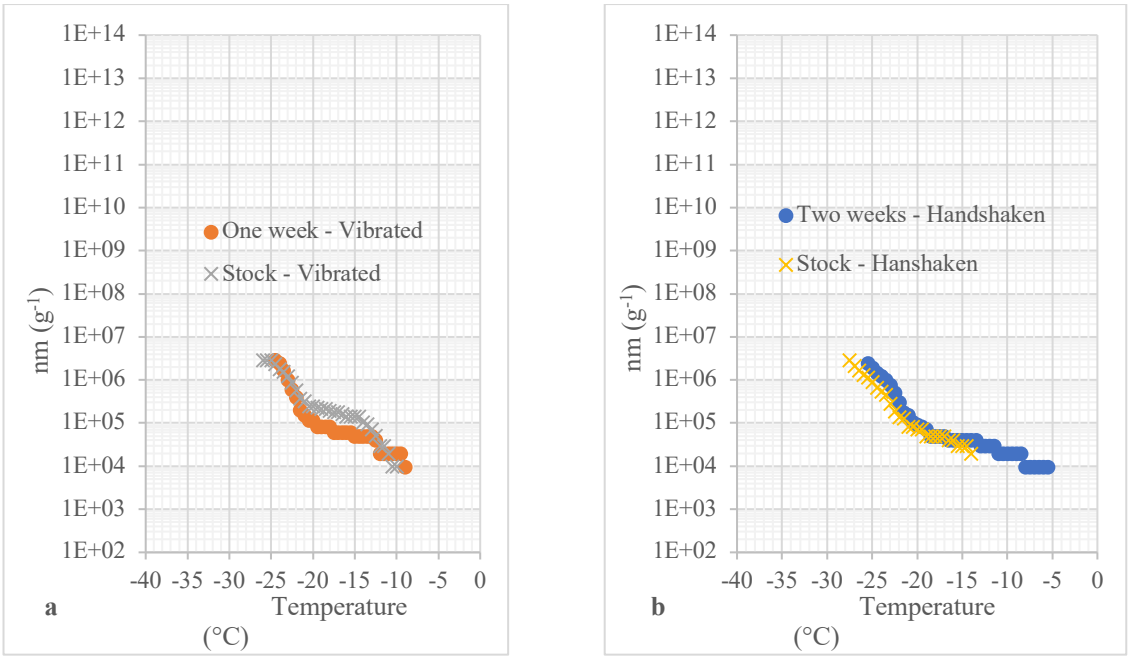

Fig. 4.7: The active site density per unit of mass of α-cellulose over a week time trial with solution (**a**) being vibrated and (**b**) being hand shaken to determine degradation as a function of time.

FC was used to confirm replication of results with the original run being conducted in May/June of 2017 and replicated in May of 2018. There was a secondary run in May of 2018 to confirm replication of the 2018 sample. Figure 4.8 shows the results of these suspensions with the greatest difference being between the first and last experiment with a difference of 1°, which was at the higher temperature (-17°C to -18°C) and could be due to artifacts that were not completely separated during the pulverization/deagglomeration process. The suspensions were recreated rather than re-used to confirm the methods handling and preparation between two technicians stayed the same. Of the three experiments, the relative standard deviation error percentile was 23.498. This showed there was no sample degradation over a year, loss of machine efficiency, nor loss in the confidence index of the results.

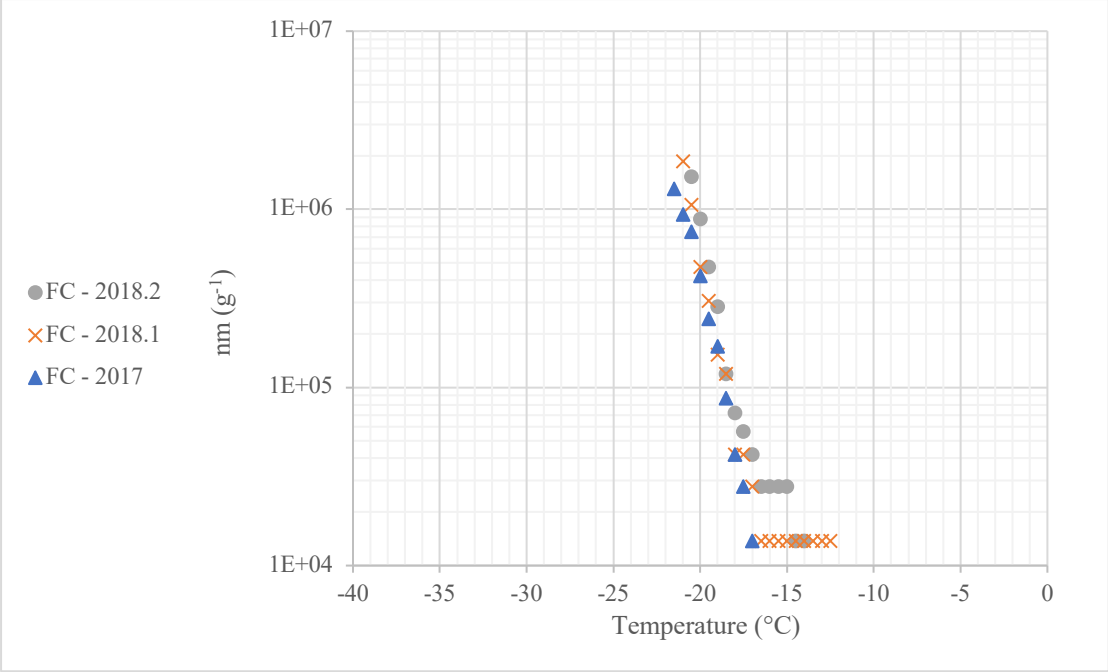

Fig. 4.8: Active site density per unit of mass of Fibrous cellulose conducted on the WT-CRAFT with a year between experiments.

4.4 WT-CRAFT vs. NiPR-CRAFT

A comparison was done on the Nippon Paper Industries samples on the WT-CRAFT (**Fig. 4.9**) and NiPR-CRAFT (**Fig. 4.10**). This was used to confirm that both machines are in agreement with each other. Another reason was to confirm that the samples were easily replicated. The powder CM-CNF had no difference between the machines with samples having an n_m of 10^8 at -25°C. As for the gel CM-CNF, there was a difference of about two orders of magnitude at -25°C [NiPR-CRAFT at 10^{10} and WT-CRAFT at 10^8]. The difference for the TEMPO-CNF short sample was about half an order of magnitude difference at -25°C [NiPR-CRAFT at 10^9 and WT-CRAFT at $10^{7.5}$]. TEMPO-CNF standard had a single order of magnitude difference at -25°C [NiPR-CRAFT at 10^8 and WT-CRAFT at 10^7].

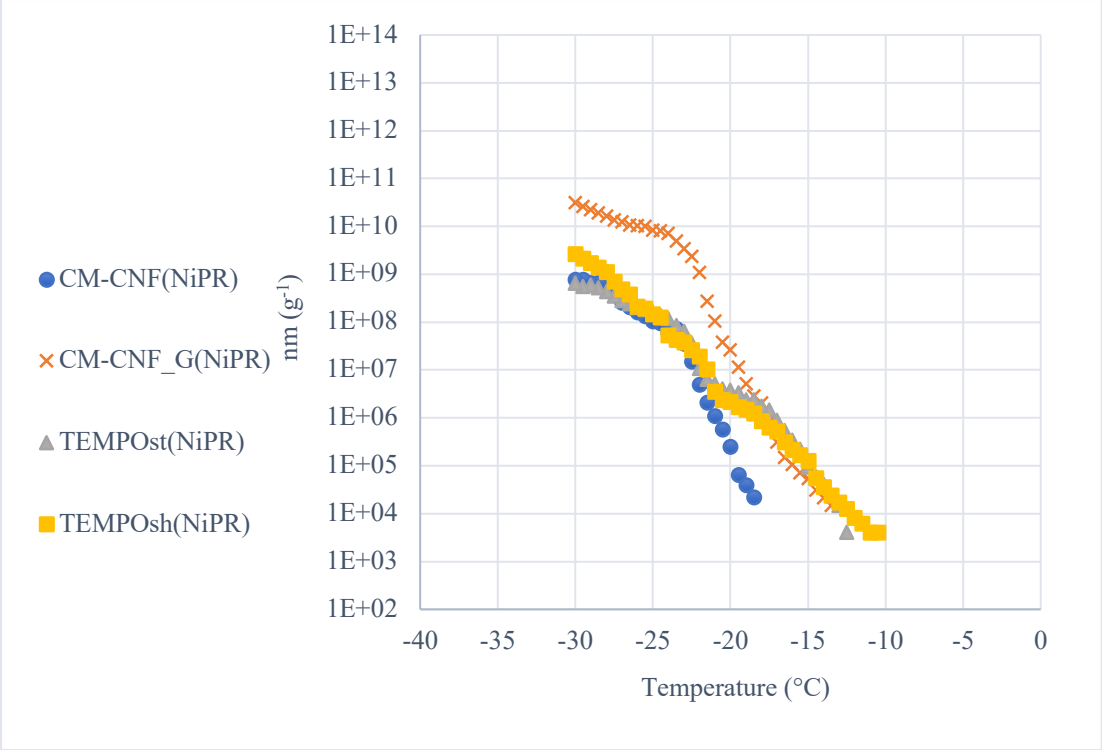

Fig. 4.9: All samples provided by Nippon Paper Industries conducted on the NiPR-CRAFT.

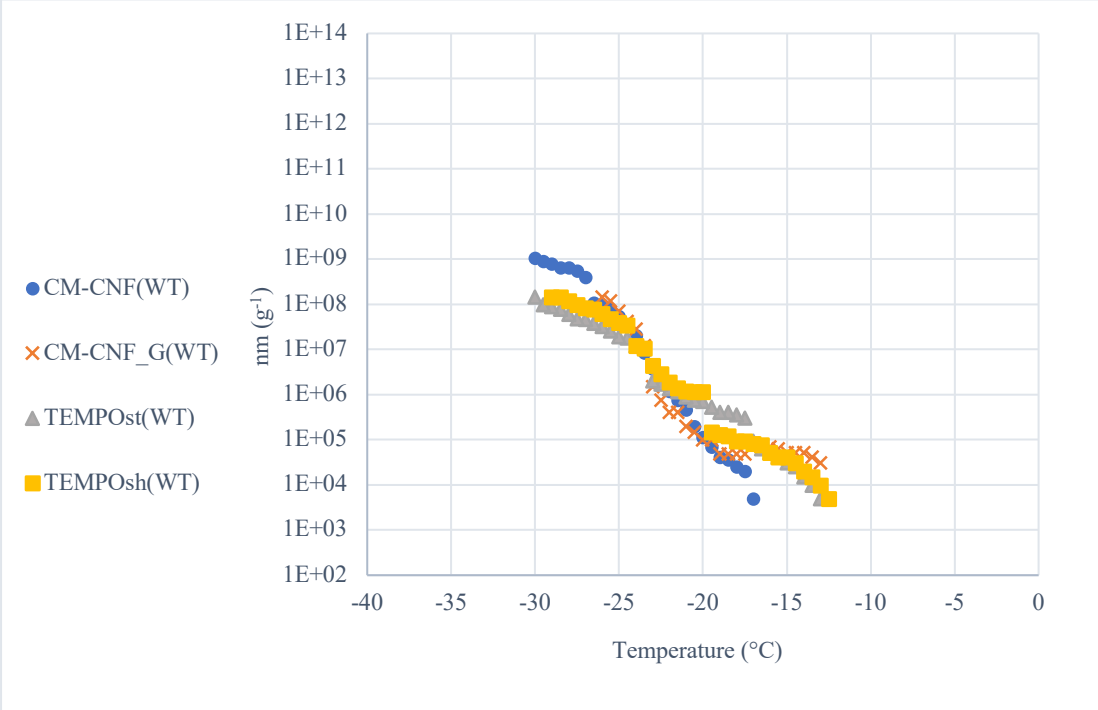

Fig. 4.10: All samples provided by Nippon Paper Industries conducted on the WT-CRAFT.

CHAPTER V

ARCTIC RESULTS

5.1 Frozen Fraction

There were ten filters collected in Ny-Ålesund, Svalbard, over the span of the month (March) in 2017. In those ten filter samples, there was a general onset of activation between -16°C and -21°C and completion by -21°C and -26°C in the original stock solution (**Fig. 5.1**). All filters were within a 5°C difference, indicating that the ice nucleating abilities of particles collected in all filters were similar with the particulates collected over varying lengths and time across the month of March in 2017. All suspension samples were generated with a stock solution that contained the filter and a set amount of water for the first droplet freezing event to correspond to n_{INP} of 0.001 (L^{-1}).

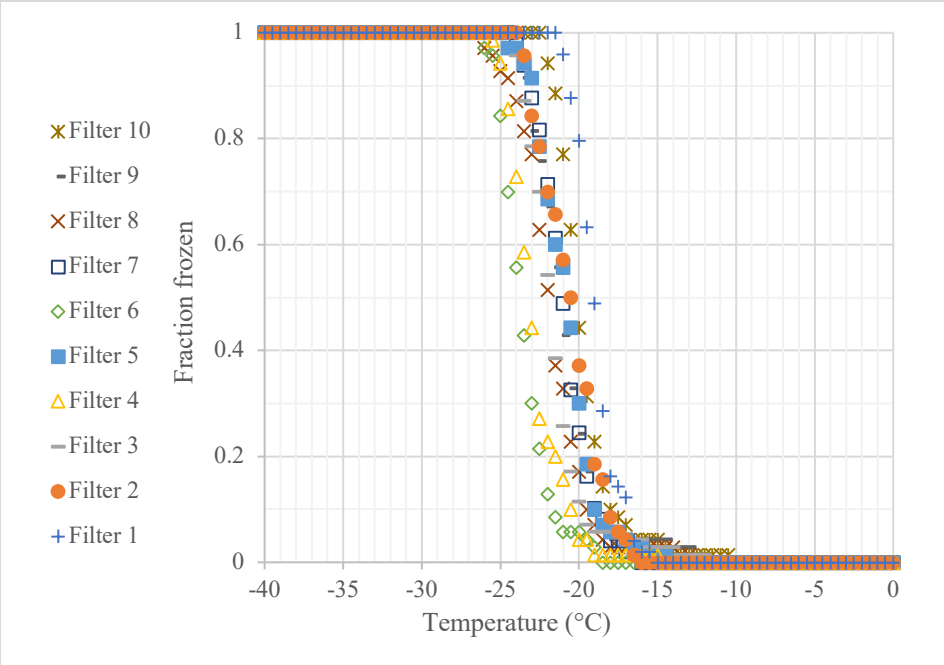

Fig. 5.1: The Fraction Frozen of all ten filters using only the stock solution.

5.2 n_{INP}

The number of INPs per volume of air was measured over the month of March 2017. The time series plot of the number of INPs were determined at three distinct temperatures: -15°C, -20°C, and -25°C (**Fig. 5.2)**. This allowed for calculation of an overall average for March 2017, which was 0.32 ± 0.07 L^{-1} at -25°C. In comparison, a study done by Schrod et al. (2017) showed the average INPs from May of 2015 to June of 2016 (**Fig. 5.3)** was 0.32 ± 0.03 L^{-1} at -25°C. The results are compatible with this study indicating that March of 2017 is typical of conditions for Ny-Ålesund, Svalbard.

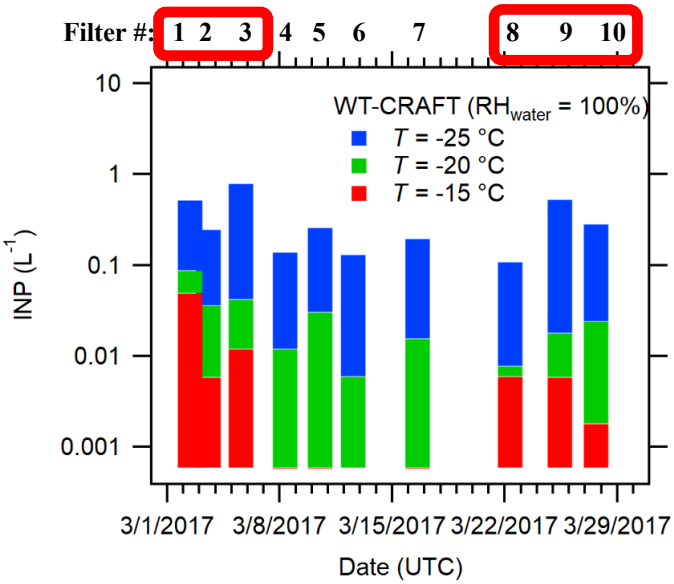

Fig. 5.2: Time comparsion of all filters from March 2017 at three destinct temperatures.

For n_{INP} (**Fig. 5.4**), all were ice nucleated up to -26°C and diluted until the overlaid results ended or passed that temperature because, after -26°C, there was higher probability of artifacts or contamination to influence the water than the filter samples themselves. It is seen that at very low temperatures, there are not enough INPs to influence to water they are placed in and artifacts or contamination will have a greater influence. All ten filters were similar in their activation per liter of air, but Arctic filter #1 shows the bimodal activation the best in its very distinct activation

curve. By -15°C, Arctic filter #1 was at 0.0401 L^{-1} while all other samples were still around 0.001 L^{-1}. Prior to -25°C, there is a wide variance between the samples, but at -25°C, the samples are within an order of magnitude of each other [0.1 to 1 L^{-1}].

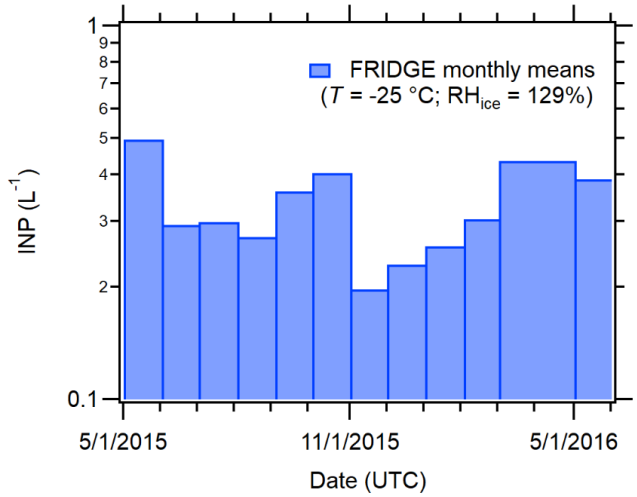

Fig. 5.3: Comparison to a previous study done by Schrod et al. (2017).

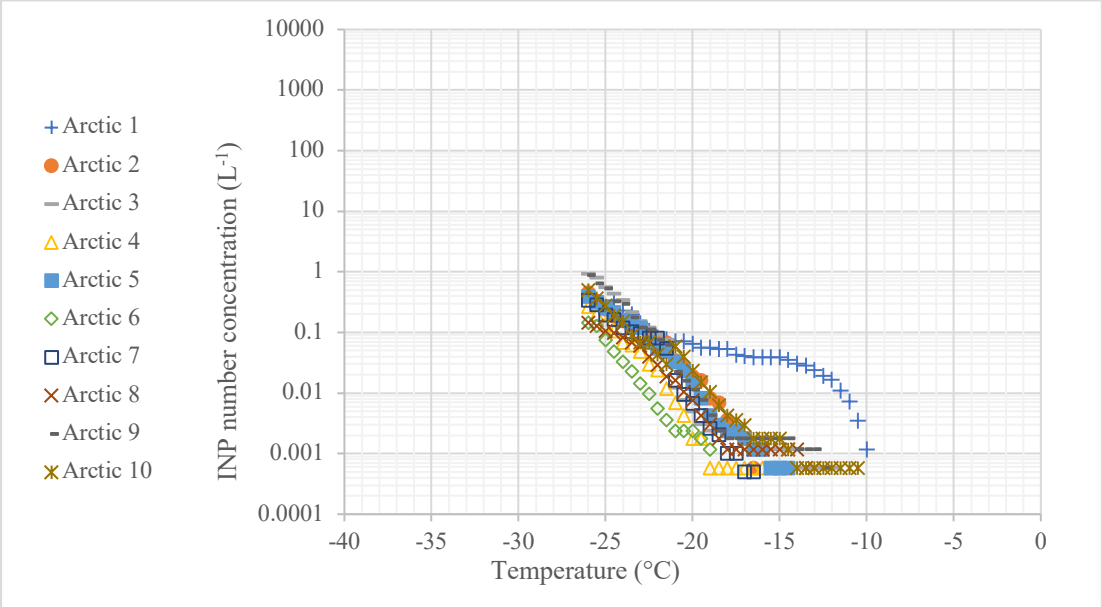

Fig. 5.4: n_{INP} of all ten nucleopore filters until to -26°C with the dilutions required.

5.3 Particle Concentrations

In March of 2017 in Ny-Ålesund, Svalbard, there were three distinct periods showing different levels of particle concentration levels: Low concentration – 47.0 cm^{-3}; Medium concentration – 93.0 cm^{-3}; and High concentrations – 195.2 cm^{-3}. Over the course of the month, the concentration levels are seen to progressively increase.

The concentration levels were seen to be affected by the wind speed and direction, temperature, pressure system, and relative humidity. In Figure 5.5, as the wind speed increased from the southwest and had a direction over 200°, the aerosol concentration increased. When the temperatures and relative humidity decreased, the concentration levels were more abundant. It was also shown that, as the month progressed, there were higher levels of particles in the range of 0.1 and 1 µm. In the D_p (µm) graph, the diameters of the aerosols are shown, and later in the month, the size distributions substantially increased with the concentration levels – ~ 0 to200 cm^{-3} at the beginning half and ~ 0 to 1000 cm^{-3}. The results of the 2017 campaign show no notable correlation between the ambient aerosol and INP concentrations.

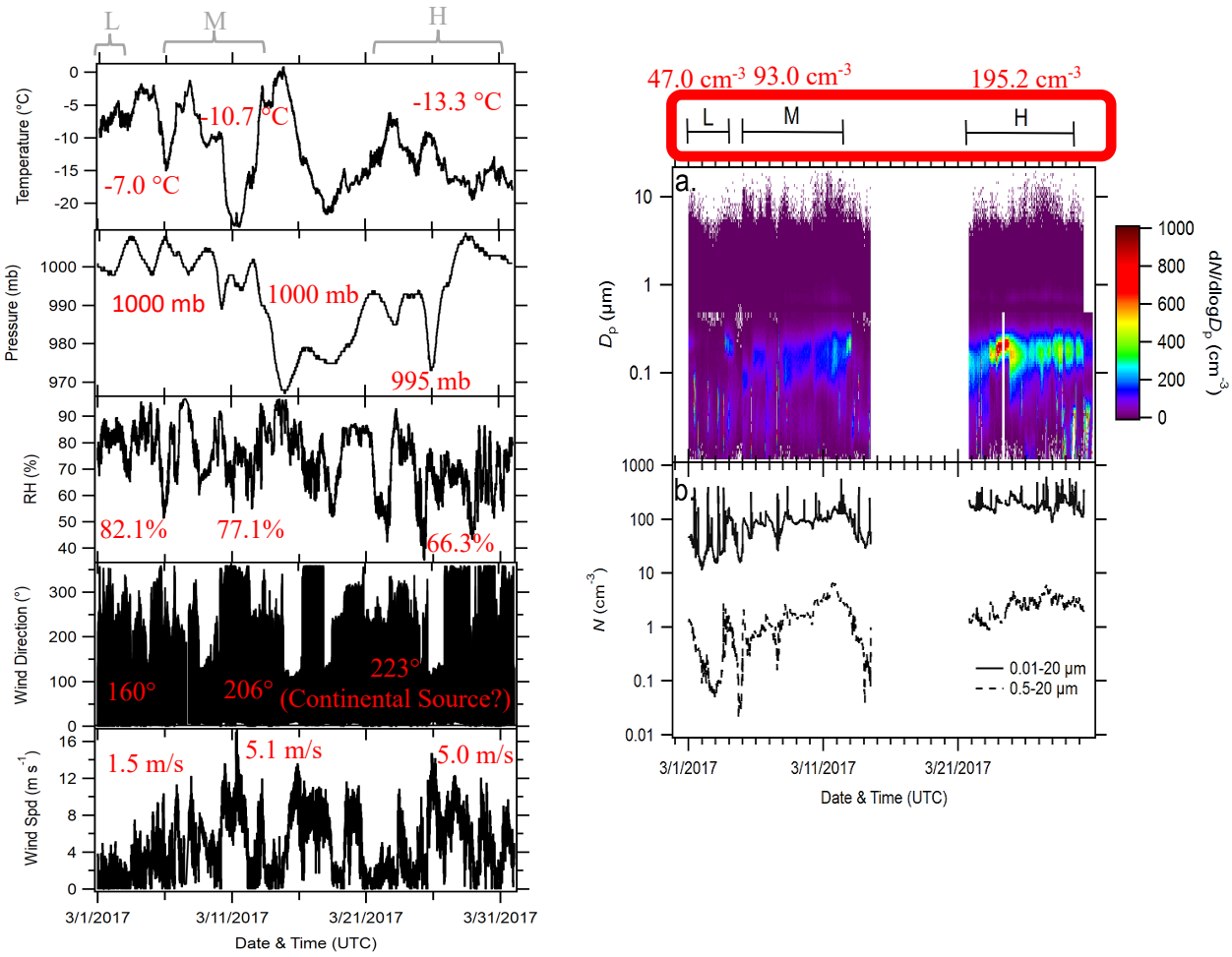

Fig. 5.5: Atmospheric conditions in relation to temperature, pressure, relative humidity, wind direction, and wind speed within the atmophere.

CHAPTER VI

DISCUSSION

6.1 Cellulose

With the data collected at both West Texas A&M University and the National Institute of Polar Research, the data for each sample were compared at three distinct degrees: -15°C, -20°C, and -25°C. In figure 6.1, the graph shows the level of concentrations at said temperatures. Within these data sets, a comparison was conducted to determine the variability between the two machines; this was done to determine whether there was a significant difference. For example, there was a difference seen between the CM-CNF samples. The CM-CNF powder had a difference in the early activation at -15°C. The samples run on the NiPR-CRAFT had activation while the samples run on the WT-CRAFT did not. This is believed to be caused by an artifact that, which has been seen to occur in samples other than just the CM-CNF powder. For example, in section 4.3 figure 4.8, the FC samples shows continues early activation of a single droplet until -17°C.

The other noticeable difference in the results were the results from the CM-CNF gel, which had a difference of two orders of magnitude. The reason for this difference could be that, at the National Institute of Polar Research, the sample had already been pre-prepared by Nippon Paper Industries. On the other hand, the CM-CNF sample that was used at West Texas A&M University was prepared at the university from the CM-CNF powder sample. Another reason that the

samples had such a big difference between them is that the sample done on the NiPR-CRAFT was created as a bulk sample while the sample done on the WT-CRAFT was created in small quantities for the intended purpose of immediate use to avoid diminishing the quantity of the CM-CNF powder. This could have influenced how many particulates were in each sample due to there being fewer in a smaller quantity rather than evenly distributed throughout a bulk sample.

Most of the samples were run multiple times to determine if the results were consistent. The samples were averaged at each temperature point. For example, in Figure 6.1, there are three temperatures chosen as comparison points, -15°C, -20°C, and -25°C. At the set temperature, all data points were collected and averaged based on those points alone.

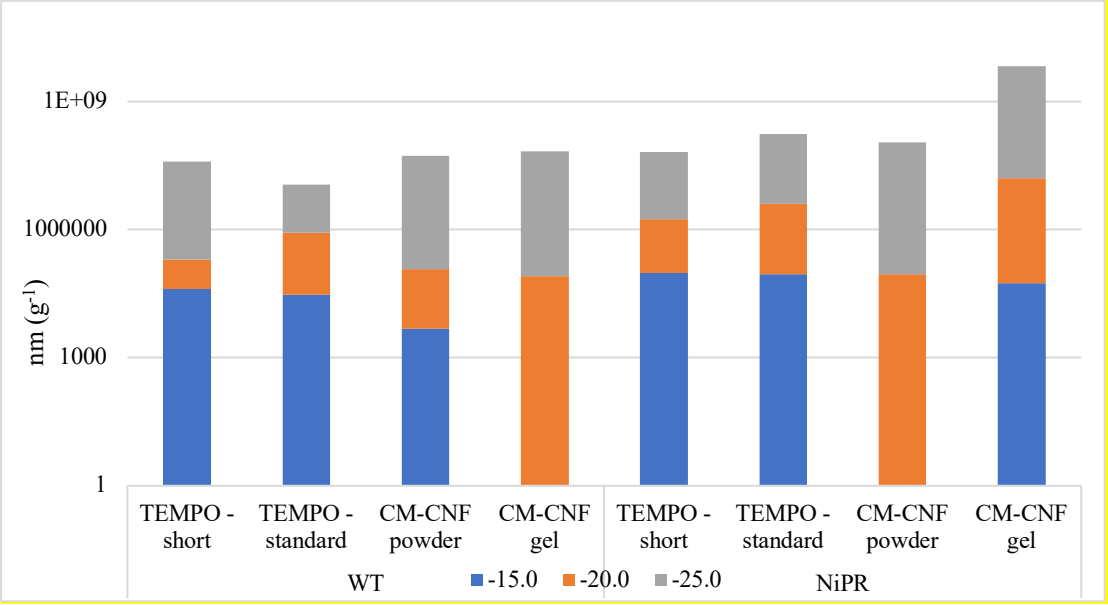

Fig. 6.1: Comparison of the two machines and concentration levels.

Microcrystalline and nanocrystalline comparison enabled me to determine if the ice nucleation efficiency is dependent on the size of the particle or if it is cause by the porous structure (Hiranuma et al., 2018). In Figure 6.2, the nanocrystalline had higher IN abilities in comparison to MCC and α-cellulose. FC and Arbo-cellulose are in the same range as the first three nanocrystalline cellulose samples. CM-CNF gel

and NCC had a greater total concentration than the rest. This further confirmed that the ice nucleation efficiency is not dependent on particle size for this data set. From these results, the hypothesis that the shorter stranded cellulose being more IN active is rejected.

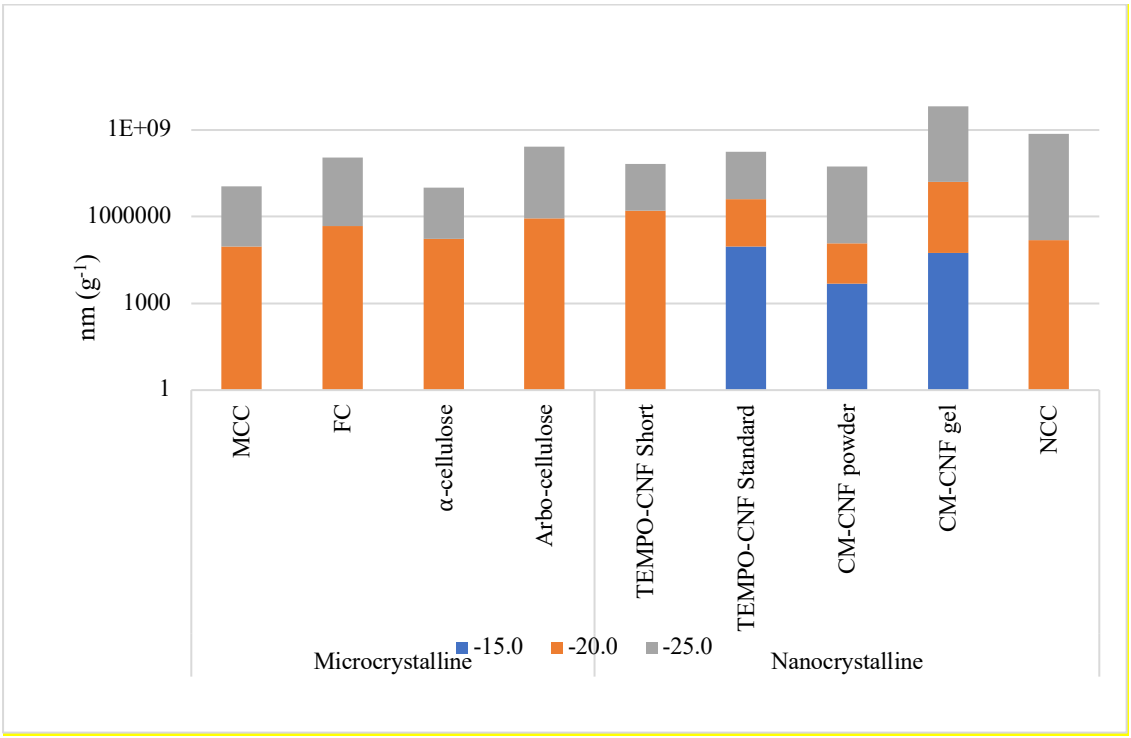

Fig. 6.2: Comparison of all microcrystalline and nanocrystalline data with the concentration levels.

In Chapter 4.2, the samples TEMPO-CNF short and CM-CNF gel were both more active than their alternates, TEMPO-CNF standard and CM-CNF powder. CM-CNF gel may have been more porous than CM-CNF powder due to the successive mechanical fibrillation, which could have exposed the samples more porous structures. The same reasoning could be applied to TEMPO-CNF short since the sample would have been through more mechanical cycles than the TEMPO-CNF standard. As stated in Hiranuma et al. (2018), the sample`s length will have less of an influence on the IN activity than the porous structure.

By using the CRAFTs, I successfully determined the effect of immersion freezing on a set volume of water droplets with a weight-based solution. This allowed

for a deeper understanding of what effect cellulose has on the atmosphere because, in the past, it has been overlooked by the monitors looking at the atmospheric implications. This study allows for a partial look at what will occur when the pre-determined weight percent is super-cooled. By doing this, the data received can be inferred for the water within a mixed-phased cloud. This project is only the beginning for determining the effects of cellulose. Once the effect of one particle per one droplet is known, a model can be generated to make a prediction based on a set number of cellulose particles within the atmosphere.

Further studies need to be done to document all different lengths and porous structures for the all-natural and synthetic types of cellulose. To fully understand the implications of cellulose, another study needs to be done to look at natural versus synthetic cellulose to determine whether plant debris or man-made products have more of an impact on ice formation. By running the synthetics though the CRAFT measurements before they are used in mass distributed products, the study would be able to determine if there would be any effects as the product degrades over time. This would help to determine which synthetic cellulose would be best to use, and by using the CRAFT, it will indicate, within a timely manner, how that specific particulate will affect the immersion freezing.

6.2 Arctic

In the Arctic samples, there were occurrences of bimodal activation. An example is A-CARE_GB_01 (seen in **Fig. 6.3**) where there is early activation at -10°C that tapers off around -20°C where there is a second activation. There is a reference line in purple to a previous study done on marine microlayers (Irish et al., 2017; Wilson et al., 2016). This reference overlays with the early activation which indicates it may be marine biogenic aerosols.

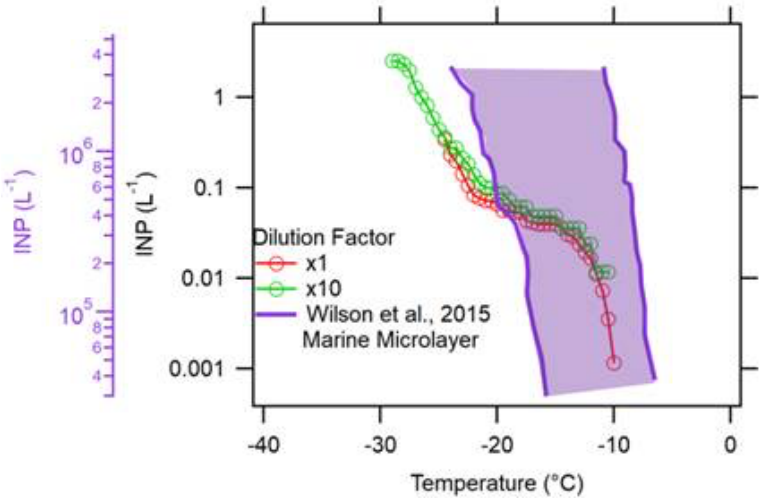

Fig. 6.3: *n*INP of Filter A-CARE_GB_01 with a bimodal activation.

This study contributed to identifying how the particles involved interacted with water vapor and supercooled water droplets. With the immersion freezing tests, the data revealed a bimodal freezing capability, which indicates that there may be marine biogenic aerosols entering into the atmosphere, but this microlayer may be small in comparison to other particulates within this region. These particulates can be carried from different areas in the ocean into the Arctic region through the ocean currents and wind direction.

This study was only based on one month`s data and compared to two other months from the previous two years. To improve the understanding of the Arctic`s atmosophere, more studies need to be done and not just one month out of the year. A study consisting of one month during each season would help to determine if this occurrence is only during the spring season, or if they are occurred during the entire year. To be able to draw a solid conclusion for the habits of the Arctic`s atmosphere, the study needs to be repeated over a couple of years to avoid any statistical sampling issues. Lastly, a biological study of what is being collected would help to determine the identity of the particulates.

CHAPTER VII

CONCLUSION

7.1 Cellulose

Cellulose particulates have been overlooked by the atmospheric modeling systems, but due to their high concentrations, they were a good candidate as a research subject. With this in mind, I used nine different types of cellulose particles, and within this project, they resulted in two clusters for the Frozen Fraction. The first cluster consisted of TEMPO-CMF short, TEMPO-CNF standard, and CM-CNF; their collective freezing rate was -11°C to -17°C. The second cluster included the rest of the nine samples, NCC, CM-CNF powder, Arbo-cellulose, FC, and MCC, with a collective freezing rate of -17°C to -23°C. The particles did not separate based on size, so it may have been due to their porous structures (Hiranuma et al., 2018). As for n_m, the results showed varying separations at -25°C that were also not solely based on particle size. Using -25°C as the set temperature, the samples separated out accordingly: 10^10 n_m g^{-1} (CM-CNF Gel – NiPR), 10^8.5 n_m g^{-1} (Arbo-cellulose), 10^8 n_m g^{-1} (CM-CNF Powder – both institutes, CM-CNF Gel – WT, TEMPO-CNF short and standard – NiPR, and FC), 10^7.5 n_m g^{-1} (TEMPO-CNF short and standard – WT), and 10^7 n_m g^{-1} (MCC and α-cellulose). The only drastic difference that was seen was between the CM-CNF gel, which had a possibility of being due to the sample being made in smaller quantities and the larger quantity being provided by a company. Therefore, the hypothesis, the idea that the shorter strands would be more

IN active than the longer strands, was rejected and failed to reject the null hypothesis that there was no difference based on the size of the cellulose strands.

The nanocrystalline cellulose was done on both the WT-CFRAFT and NiPR-CRAFT. This was to confirm sampling techniques, as well as the consistency of both machines, were the same at both the host and WTAMU. To confirm that there was no significant difference between the machine and their perspective results, a comparison on concentrations was done at three set temperatures (-15°C, -20°C, and -25°C) for four of the nanocrystalline cellulose samples (CM-CNF powder, CM-CNF gel, TEMPO-CNF short, and TEMPO0CNF standard). There were two notable differences on the CM-CNF samples. The first difference is the powder at -15°C. Samples run on the NiPR-CRAFT shows a concentration level, but the WT-CRAFT does not. That difference leads to the assumption that there was an artifact. The most notable difference coming from the CM-CNF gel, which as previously stated, may have been different due to product creation and number of particles but liter.

Another comparison that was done is time trials. These time trials were conducted to determine three things: 1) sample preparation and experiment consistency between multiple technicians; 2) sample degradation; and 3) loss of machine efficiency over time machine. The first time-trial was done on α-cellulose to determine if there was a loss of degradation over a week to two-week period. This sample was made with two different techniques to confirm that there was no significant difference between distribution methods. The other time-trial was based over a year with the FC sample. This sample was used by two technicians and found that there was no degradation of the original sample over that time. It was also found

that the sample technique was repeatable. Not only did this show that the results are replicable between different technicians, but it also showed that the WT-CRAFT has no loss of efficiency with rapid continued use over a year long period.

7.2 Arctic

The samples collected in Ny-Ålesund, Svalbard, in March of 2017 had a consistent Frozen Fraction rate for all ten filters. There was an initial onset of freezing between -16°C and -21°C, and all droplets were frozen between -21°C and -26°C. The number of particles within a unit of air was calculated, which was around 0.1 and 1 L^{-1} for all ten filter samples. It was seen that there was a distinct increase in concentrations at the beginning and end of the month as well as particulates causing the water to freeze at the higher temperature (-15°C). Some of the reasons that these concentrations were affected were due to the low temperatures, low pressure, and relative humidity. To validate these results, the samples were compared to a previous study that occurred in May and June of 2015 and 2016. The said study had an average concentration of 0.32 ± 0.03 L^{-1} at -25°C, while this study had an average of 0.32 ± 0.07 L^{-1}. These samples were in agreement with only an average difference of 0.04 L^{-1}.

There have not been many studies done on the particulates from the Arctic, but there is much need for them. The results of this study showed that there are potentially marine biogenic aerosols, shown through the bimodal activation, that were collected. Marine biogenic aerosols are important because they freeze at relatively higher temperatures (-10°C) than some of the other ambient particulates. These

particulates may be coming from pollution produced in the upper hemisphere, but further studies need to be done to confirm the severity of these particulates.

The Arctic is an important study site because there is not a lot of human interference with the particulate concentrations, but research can still be done on the particulates that are trapped within the snow and glaciers. These allow for research to be conducted on what is being spread throughout different regions, what method are they being transported, and how much effect the particulates have on the atmosphere. The Arctic is an important region that, if possible, should be continued to study throughout different times of year to determine the seasonal variation. A study that should be conducted to determine if the high concentrations at the beginning and end of the month are singular occurrences or if they will continue to occur throughout the following months. Another study that should be conducted is a comparison between the two poles to find if it is solely based on the pollution coming from the Northern hemisphere of if there needs to be further studies into what is specifically occurring with the marine biogenic aerosols.

LITERATURE CITED

Abdul Khalil, H. P. S., Davoudpour, Y., Islam, N. Md., Mustapha, A., Sudesh, K., Dungani, R., & Jawaid, M. Production and modification of nanofibrillated cellulose using various mechanical processes: A review. *Carbohydrate Polymers* **99**, 649-665 (2014).

ARASH AZMA 2: Arbocel Natural Cellulose Fiber: http://arashazma2.com/Arbocel.htm, last access: 21 March 2019.

Bauman, R. W. in *Microbiology with diseases by taxonomy* (5th Edition) Ch. 6 (Pearson Education Inc, 2017).

Boucher, O. et al. in *Climate Change 2013: The Physical Science Basis* (eds Stocker, T. F. et al.) Ch. 7 (IPCC, Cambridge University Press, 2013).

Christner, B. C., Cai, R., Morris, C. E., McCarter, K. S., Foreman, C. M., Skidmore, M. L., Montross, S. N., & Sands, D. C. Geographic, seasonal, and precipitation chemistry influence on the abundance and activity of biological ice nucleators in rain and snow. *Proceedings of the National Academy of Sciences of the United States of America* **105**, 18,854-18,859 (2008).

Cohen, J., Screen, J. A., Furtado, J. C., Barlow, M., Whittleston, D., Coumoiu, D., Francis, J., Dethloff, K., Entekhavi, D., Overland, J., & Jones, J. Recent arctic amplifiocation and extreme mid-latitude weather. *Nature Geoscience* **7**, 627-637 (2014).

DeMott, P. J. in *Cirrus*, edited by: Lynch, D. K., Sassen, K., Starr, D. C., and Stephens, G. 102-135 (Oxford University Press, 2002)

DeMott, P. J., Hill, T. C. J., Petters, M. D., Bertram, A. K., Tobo, Y., Mason, R. H., Suski, K. J., McCluskey, C. S., Levin, E. J. T., Schill, G. P., Boose, Y., Rauker, A. M., Miller, A. J., Zaragoza, J., Rocci, K., Rothfuss, N. E., Taylor, H. P., Hader, J. D., Chou, C., Huffman, J. A., Pöschl, U., Prenni, A. J., & Kreidenweis, M. Comparitive measurements of ambient atmospheric concentrations of ice nucleation particles using multiple immersion freezing methods and a continuous flow diffusion chamber. *Atmospheric Chemistry and Physics* **17**, 11227-11245 (2017).

Després, V. R., Huffman, J. A., Burrows, S. M., Hoose, C., Safatov, A. S., Buryak, G., Fröhlich-Nowoisky, J., Elbert, W., Andreae, M., O., Pöschl, U., & Jaenicke, R. Primary biological aersol particles in the atmosphere: A review. *Tellus B: Chemical and Physical Meteorology* **64**, 1-58 (2012).

Dumka, U. C., Moorthy, K. K., Kumar, R., Hegde, P., Sagar, R., Pant, P., Singh, N., & Babu, S. S. Characteristics of aerosol black carbon mass concentration over a high-

altitude location in the Central Himalayas from multi-year measurements. *Atmospheric Research* **96**, 510-521 (2010).

Hartmann, S., Niedermeier, D., Voigtländer, J., Clauss, T., Shaw, R. A., Wex, H., Kiselev, A., & Stratmann, F. Homogeneous and heterogeneous ice nucleation at LACIS: operating principle and theoretical studies. *Atmospheric Chemistry and Physics* **11**, 1753-1767 (2011).

Hiranuma, N., Möjhler, O., Yamashita, K., Tajiri, T., Saito, A., Kiselev, A., Hoffmann, N., Hoose, C., Jantsch, E., & Murakami, M. Ice nucleation by cellulose and its potential contribution to ice formation in clouds. *Nature Geoscience* **8**, 273-277 (2015).

Hiranuma, N., Adachi, K., Bell, D., Belosi, F., Beydoun, H., Bhaduri, B., Bingemer, H., Budke, C., Clemen, H.-C., Conen, F., Cory, K., Curtius, J., DeMott, P., Eppers, O., Grawe, S., Hartmann, S., Hoffmann, N., Höhler, K., Jantsch, E., Kiselev, A., Koop, T., Kulkarni, G., Mayer, A., Murakami, M., Murray, B., Nicosia, A., Petters, M., Piazza, M., Polen, M., Reicher, N., Rudich, Y., Saito, A., Santachiara, G., Schiebel, T., Schill, G., Schneider, J., Segev, L., Stopelli, E., Sullivan, R., Suski, K., Szakáll, M., Tajiri, T., Taylor, H., Tobo, Y., Weber, D., Wex, H., Whale, T., Whiteside, C., Yamashita, K., Zelenyuk, A., and Möhler, O.: A comprehensive characterization of ice nucleation by three different types of cellulose particles immersed in water: lessons learned and future research directions. *Atmos. Chem. Phys. Discuss*., https://doi.org/10.5194/acp-2018-933, in review, (2018).

Hoose, C., Lohmann, U., Erdin, R., & Tegen, I. The global influence of dust mineralogical composition on heterogeneous ice nucleation in mixed-phase clouds. *Environmental Research Letters* **3**, 1-14 (2008).

Irish, V. E., Elizondo, P., Chen, J., Chou, C., Charette, J., Lizotte, M., Ladino, L. A., Wilson, T. W., Gosselin, M., Murray, B. J., Polishchuk, E., Abbatt, J. P. D., Miller, L. A., Bertram, A. K. Ice-nucleating particles in Canadian Arctic sea-surface microlayer bulk seawater. *Atmospheric Chemistry and Physics* **17** 10583-10595 (2017).

Isogai, A., Saito, T., & Fukuzumi, H. TEMPO-oxidized cellulose nanofibers. *Nanoscale* **3**, 71-85 (2011).

Kanji, Z. A., Ladino, L. A., Wex, H., Boose, Y., Burkert-Kohn, M., Cziczo, D. J., & Krämer, M. Meteorological Monographs. *American Meteorological Society* **58**, 1.1-1.33 (2017).

Kerminen, V. Relative roles of secondary sulfate and organics in atmospheric cloud condensation nuclei production. *Journal of Geophysical Research* **106**, 17,321-17,333 (2001).

Koop, T., Luo, B., Tsias, A., & Peter, T. Water activity as the determinant for homogeneous ice nucleation in aqueous solutions. *Nature* **406**, 611-614 (2000).

Lohmann, U. & Diehl, K. Sensitivity studies of the importance of dust ice nuclei for the indirect aerosol effect on stratiform mixed-phase clouds. *Journal of the Atmospheric Sciences* **63** 968-982 (2006).

Melodea Bio Based Solutions: Cellulose Nano Crystals Overview: http://www.melodea.eu/Default.asp?sType=0&PageId=104256, last access: 31 July 2018.

Murray, B. J., Broadley, S. L., Wilson, T. W., Atkinson, J. D., & Wills, R. H. Heterogeneous freezing of water droplets containing kaolinite particles. **11**, 4191-4207 (2011).

Prospero, J. M. Long-term measurements of the transport of African mineral dust to the southeastern United States: Implication for regional air quality. *Journal of Geophysical Research* **104**, 15917-15927 (1999).

Quiroz-Castañeda, R. E. & Folch-Mallol, J. L. *Sustainable Degradation of Lignocellulosic Biomass – Techniques, Applications and Commercialization* Ch. 6 (InTech, 2013).

Schrod, J., Weber, D., Hamilton, D., Thomson, E. S., Pöhlker, C., Saturno, J., Artaxo, P., Clouard, V., Curtius, J., Bingemer, H. Ice nucleating particles from a large-scale sampling network: insight into geographic and temporal variability. EGU Poster (2017).

Serreze, M. C. & Barry, R. Process and impacts of Arctic Amplification: A research synthesis. *Global and Planetary Change* **77**, 85-86 (2011).

Takemura, T., Nozawa, T., Emori, S., Nakajima, T. Y., & Nakajima, T. Simulation of climate response to aerosol direct and indirect effects with aerosol transport-radiation model. *Journal of Geophysical Research* **110**, 1-16 (2005).

Tobo, Y. An improved approach for measuring immersion freezing in large droplets over a wide temperature range. *Scientific Reports* **6** (2016).

Welti, A., Kanji, Z. A., Lüönd, F., Stetzer, O., & Lohmann, U. Exploring the mechanisms of ice nucleation on kaolinite: From deposition nucleation to condensation freezing. *Journal of the Atmospheric Sciences* **71** 16-36 (2014).

Wilson, T. W., Ladino, L. A., Alpert, P. A., Breckels, M. N., Brooks, I. M., Browse, J., Burrows, S. M., Carslaw, K. S., Huffman, A., Judd, C., Kilthau, W. P., Mason, R. H., McFiggans, G., Miller, L. A., Nájera, J. J., Polishchuk, E., Rae, S., Schiller, C. L., Si, M., Temprado, J. V., Whale, T. F., Wong, J. P. S., Wurl, O., Yakobi-Hancock, J. D., Abbatt, J. P. D., Aller, J. Y., Bertram, A. K., Knopf, D. A., Murray, B. J. A marine biogenic source of atmospheric ice-nucleating particles. *Nature* **525** 234-238 (2015).

APPENDIX A

ACRONYMS & UNITS

Acronym	Description	Unit	Description
α	alpha	**cm**	centimeters
β	Beta	**cm^{-3}**	cubic centimeter
CCN	cloud condensation nuclei	**g**	gram
CFDC	continuous flow diffusion chamber	**hPa**	hectopascal
C_m	mass concentration of the particles in the solution	**kDa**	kiloDalton
CM-CNF	Carboxymethylation Cellulose	**L**	Liter
CRAFT	Cryogenic Refrigerator Applied Freezing Test	**lpm**	Liter per minute
CS	cold stage	**m**	meter
d	dilution ratio	**$m\ s^{-1}$**	meter per second
D_p	diameter of the particle	**m^{-2}**	square meters
F. avenaceum	*Fusarium avenaceum*	**m^{-3}**	cubic meter
FC	Fibrous Cellulose	**mb**	millibars
f_{frozen}	number frozen droplets	**mm**	mili-meter
$f_{unfrozen}$	number unfrozen droplets	**MΩ**	milliohm
IN	Ice nucleating	**ng**	nano-grams
INPs	Ice-nucleating particles	**nm**	nano-meters
INUIT	Ice Nuclei research UnIT project	**Tg**	Teragrams
IS	ice Spectrometer	**vlpm**	volume of liter per minute
K-feldspar	Potassium-Feldspar	**W**	Watts
MCC	Microcrystalline Cellulose	**wt %**	weight percent
MOUDI-DFT	micro-orifice uniform deposit impactor-droplet freezing technique	**yr**	year
M_{Total}	total mass	**µg**	micro-gram
N	number	**µL**	micro-Liter
NaCl	Sodium Chloride	**µm**	micro-meters
NCC	Nanocrystalline Cellulose		
n_{INP}	number of ice-nucleating particles		

NiPR	National Institute of Polar Research
NiPR-CRAFT	National Institute of Polar Research - Cryogenic Refrigerator Applied Freezing Test
n_m	active site density per unit mass
n_s	active site density per unit surface area
P. syringae	*Psuedomonas syringae*
RH_i	relative humidity of ice
RH_{water}	relative humidity of water
S_{total}	total surface
T	Temperature
TEMPO-CNF	2,2,6,6-tetramethylpiperidine-1-oxyl Cellulose Nanofibers
TSP	Total Suspended Particles
UTC	Universal Time Coordinated
V_{drop}	volume of the droplet
V_s	sampled volume of air
V_w	volume of liquid
WT-CRAFT	West Texas A&M University - Cryogenic Regrigerator Applied Freezing Test
WTAMU	West Texas A&M University

SUPPLEMENTARY DOCUMENTS

CRAFT MANUAL

SAMPLE PREPARATION

Powder

1. Before going to weigh the sample, make sure all desired materials are within the carrying bag.
    - This includes all tubes, samples, gloves, isopropyl, parafilm, spoon, and pipette and tips you will be using during this process.
2. Turn on the microbalance scale and confirm that the scale is balanced.
    - On the back, there is a circle with a bubble. Make sure the bubble is in the absolute center of the circle to achieve the most accurate weight.
3. Place a Falcon tube with stand on the scale and zero out the scale.
4. Clean the spoon with isopropyl and a Kimwipe two to three times.
5. Scoop a small estimated amount of material into the Falcon tube and wait until weighed amount levels out.
    - If weight is over the desired amount, remove portion of sample from tube using the stainless-steel spatula and discard on a kimwipe.
        i. ****Never** place sample back into the original container after it has been removed.
6. Continue until the desired weight has been reached, pipette the pre-calculated amount of water into the Falcon tube to create the desired weight percent.
7. Shake sample for 1 minute to distribute the sample into the water.
8. Clean all utensils with isopropyl and a Kimwipe.
9. Parafilm lid of the Falcon tube to prevent any loss of sample.
10. Place all materials back into the storage bag and throw away any materials into the
11. Turn off microbalance scale and clean the scale with isopropyl and a kimwipe.
12. When returned to the lab, place all samples in a 4ºC refrigerator until needed.

Filter

1. Remove cover from the designated Prep Station.
2. Clean the base of the Prep Station twice with isopropyl and Kimwipes.
3. Place fresh Aluminum foil down so that it covers the entire area
    a. This is in case the filter does not land inside the Petri-dish
4. Clean both the tweezers and scissors with isopropyl and Kimwipes twice
    a. When placing them down, hang them off of the pipette tip case so that they do not come into contact with any other surface before touching the filter.
5. Place a new sterile Petri-dish on the Aluminum foil.
    a. The filter will be placed inside during the cutting process.
6. Remove the lid of the Filter container and use the tweezers to pick up the filter by the very most edge and place within the Petri-dish

    a. The shiny side of the filter should always be up. All particulates will be on this side.
7. Pick the Filter up with your tweezer in your non-dominant hand and cut the filter down the middle with your dominant hand.
    a. Make this cute as clean and straight as possible. You want 50% of the filter to go back into the container for later testing.
8. Place the half of the filter still held by the tweezers back into the Filter container. The other half should be in the Petri-dish where it landed.
    a. If it landed outside of the Petri-dish, pick the filter up by the very edge and place back within the Petri-dish. Remember to always place any utensils so that they are hanging
9. Once the half that is being saved is placed within the Filter container, close the lid and set it aside. Pick up the other half and cut it into four pieces - like a pie - and be sure to only touch the filter by the outermost edge.
10. Place all four filter pieces into a sterile Falcon tube with a stand
    a. Place them far into the tube because, when you open the tube, the filters will come up towards the top. May need two tweezers to get the filter into the tube.
11. Place the Filter container back into the bag it came in and place in a 4°C refrigerator and throw away the Petri-dish.
    a. Never reuse a Petri-dish.
12. Pipet the required amount of water into the pipet.
    a. Always place the filter in first. You can recover the filter if it has not had water introduced.
    b. Make sure the amount is relevant to the amount of filter used. If the calculation was done using the entire filter, adjust so that it is calculated for just the portion used.
13. Shake the tube to get the pieces of filter to the bottom and immersed within the water.
14. Shake for ten minutes with a hard shake every minute.
    a. The hard shake is to move any potential particles at the top of the Falcon tube to the bottom with the rest of the particules.
15. Let sample settle for five minutes.
    a. This allows larger particles to settle to the bottom of the sample and the atmospherically relevant particles to stay suspended within the top layer.
16. Place parafilm around lid and store sample in 4°C refrigerator until ready to use.
17. Clean up area and utensils with isopropyl and kimwipes two to three times and dispose of the Aluminum foil.

WT-CRAFT START UP

1. Switch on the Main Power Switch, located on the right-hand side of the Cryo Porter and the CRAFT will boot up
2. On PcPad main menu, select 2: Fixed Program [ENT]
    a. ‘Fixed Program’ means that the machine will stay at a constant temperature based on what is typed into the system
3. Type 5 on keypad for the SV control, Press [START]
    a. This will cool CRAFT to 5.0℃ at a rate of 1℃ per minute
    b. WT-CRAFT should be resting at a temperature of 5.0℃ prior to any experiments
4. Remove Foil Cover from acrylic top plate
5. Turn on LED light
6. Open/Turn on Computer

7. Start the OBS Studio software. Check webcam visuals for clear imaging before starting experiments

PLATING SAMPLE

1. First, wash hands and put on Nitrile Powder-free gloves
2. Clean the aluminum base plate thoroughly with Isopropyl alcohol and Kimwipes (>4x)
    a. Spray Isopropyl onto Kimwipe and proceed to cleaning plate
    b. Always end with wiping in on direction (like you would clean your car window)
    c. Be sure to check for any left-over artifacts, such as Vaseline or Kimwipe debris
    d. Never reach directly over the plate once cleaned
3. Clean plastic spatula with Isopropyl alcohol and Kimwipe (2x)
    a. Spray Isopropyl to cover spatula
    b. Use Kimwipe to clean to one direction – making sure to clean around the raised edges
    c. Inspect spatula for any leftover Vaseline
    d. Do not set spatula down once cleaned
4. Using the spatula evenly spread Vaseline on aluminum base plate (Avoid spreading to the edge of plate – leave ~1/2")
    a. Do not place lid face down and place secondary lid face up into the lid, if applicable
    b. Once Vaseline is on spatula, place lid back on to avoid contamination (**never leave Vaseline lid open**)
5. Choose appropriate Eppendorf Pipette for droplet distribution
    a. Dark Grey = 0.1 – 2.1µL
    b. Light Grey = 0.5 – 10 µL
    c. Yellow = 10 – 100 µL
    d. Turquoise = 1 – 10 mL
    e. EP tips tray is color coded to corresponded pipette
6. Adjust Pipette using the top turn dial for desired droplet size
7. Using Pipette, press down on appropriate Pipette tip with a gentle force to secure tip to Pipette
8. Pipette the prepared suspension in a uniform manner on aluminum plate with Vaseline (ex: 5x7 = 35 droplets; 7x7 = 49 droplets; 7x10 = 70 droplets)
    a. When pipetting, hold sample and lid in non-dominant hand and pipette using dominant hand
        i. If you are right handed, pipette left to right. If you are left handed, pipette from right to left
        ii. This is to avoid ever bringing anything back over the droplets once placed
    b. Inspect droplets from a distance to make sure even distribution, droplet size, and amount
        i. When placing droplets, be sure to space appropriately where droplets do not contact each other (~ 1 mm apart)
    c. <u>DO NOT</u> remove plate from hood to place in CRAFT
9. Remove CRAFT acrylic cover (only touching the edge) toward the back of the CRAFT resting the edge against the Styrofoam ring
    a. Do not place flat against the lid of Cryo Porter

10. Check that temperature sensors are vertically placed, and the sensor bar is placed parallel from the bottom on Styrofoam
11. Carefully place aluminum base plate at an angle into CRAFT (~ 45-60°) then align to the right edge
12. Fit the aluminum strip with temperature sensor attachment in the left edge pressing down along sensor to confirm complete contact
13. Rotate the temperature sensor gauge to face upward towards web camera
14. Cover the CRAFT with acrylic cover to avoid ambient contamination
15. Allow for aluminum plate and sensors to cool to [5.0℃]
16. Check cameras and lighting on computer screen to confirm proper visual

STARTING EXPERIMENT

1. On PcPad, press [ESC] to return to main menu
    a. The main menu will have two options
        i. 1: Program Control
        ii. 2: Fixed Program
2. Select '1: Program Control'
3. Choose '1: Select Program' and [ENT]
4. Use cursor to choose desired program and press [ENT]
    a. This screen has four options
        i. PRG.1: 5C – For unknown
        ii. PRG.2: -5C – For anything that freezes at -10 or below
        iii. PRG.3: -10C – Only for Pure water
        iv. Cool (2C/min) – No relevance to undergrads
5. Press [START] to begin program
    a. Green flashing dot will appear, indicating cooling on Cryo Porter
    b. Green number on Cryo Porter are the desired temperature
    c. Red numbers on Cryo Porter are the current temperature
    d. Program will reach temperature chosen and sit for 5 minutes before decreasing to AIM temperature (-38℃)
6. Program will reach temperature chosen and sit for 5 minutes before decreasing to AIM temperature (-38℃)

CRAFT LOG BOOK

1. This Log book should be located with the computer attached to the CRAFT via the webcam.
    a. Always be sure to leave this notebook with the computer.
2. Open the book to the page last written on and either draw a line, or make sure that there is already one, to separate the last log from the new one.
3. Place the sample name at the top and underneath the previous line and underline it.
    a. To the side, either write the dilution factor or the volumes used to create the suspension.
4. One the left side, write set sample (volume of droplet x # of droplets), start (program temp), and stop.
    a. These should be in a column with space on the left for timestamps for each step.
    b. Set sample timestamp is the time of the first droplet being placed onto the vaseline.
    c. The timestamp for the start time is the time when the recording is started
        i. This gives the time of when the first droplet has been laid and the start of the freezing experiment.

    d. The timestamp for the stop is when the recording is stopped.
5. On the right side, write video and data.
    a. For the video, write down the date in the format of year, month, then date (e.g., 20180215), and then place a letter after for the video of the day (ex: a = 1st, b = 2nd, etc.)
    b. For data, this will consist of two lines.
        i. The first line should be the student ID tag (assigned to you), experiment number, and the sample.
        ii. The second line should be the file name that this will be saved under and the tab colour.
6. At the very bottom, have a notes section for anything significant that has been observed.

RECORDING DATA

1. Using OBS Studio Software, hit [record] after the 5 minute countdown
    a. Scene 1 will have two sources
        i. Source 1: OptiTech Scope
        ii. Source 2: LogiTech Cam
    b. Make use both windows and cameras appear on screen
2. On the OBS Software in the bottom right hand panel labeled controls, the option to start recording
3. Use Excel file to record number of droplets frozen at the temperature frozen [Proceed to DATA ANALYSIS for further details]
4. Once all droplets are frozen, STOP recording by pressing the Stop Recording button
5. Video will compress (time consuming)
    a. Proceed to FINISHING EXPERIMENT to warm up the CRAFT for clean up
6. Recordings are located in the (CRAFT Microscope video) folder on Desktop
7. Rename video recording accordingly
    a. Label it the date and in letter sequence (ex: 20180315b – means second video recorded on the 15th of March in 2018)
8. Close computer and unplug charger

FINISHING EXPERIMENT

1. Press [ESC] on PcPad until main menu
2. Select 2: Fixed Control [ENT]
3. Type 5 on the keypad for the SV control, Press [START]
4. Wait until aluminum plate warms to 5.0℃ and All droplets are unfrozen
5. Put on Nitrile gloves
6. Remove acrylic CRAFT cover and set along back of CRAFT
7. Rotate temperature gauge (clockwise) to face back edge of CRAFT
8. Pick up aluminum plate with temperature sensor attachment and place on Styrofoam ledge
9. Slide aluminum base plate to left and pick up to remove plate from CRAFT
10. Place aluminum base plate to preparation area
11. Cover CRAFT with acrylic plate
12. Use scraper to clean off droplets and Vaseline from aluminum plate
13. Use Kimwipes and Isopropyl alcohol to finish cleaning aluminum plate
14. Turn off main power switch to CRAFT
    a. NEVER leave aluminum base plate in CRAFT when finished
15. Return to RECORDING DATA section
16. Cover Acrylic plate with aluminum cover

VIDEO ANALYSIS

1. Open the designated video file and excel spreadsheet that has been indicated within the Log book.
2. At the top of the file, confirm that all the parameters are set with the proper information.
    a. Fill in the following:

Parameters: these are held at the top of the file near the center

This box indicates the volume of droplets in microliters

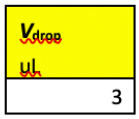

This box indicates the number of droplets used in the video

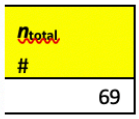

This box indicates the mg divided by the mL

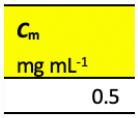

This box is the dilution factor from the sample

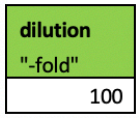

This area is the concentration mg/mL multiplied by the dilution
To get the weight percent, multiply by 10

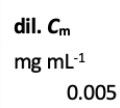

3. In the second column starting from the left, the numbers you will be inputting will go here.
    a. The numbers inputted in this column are the number of droplets that have been observed frozen.
        i. This should coordinate with the temperature on the left of it.
    b. Insert zeros until the temperature for the start of the program selected.
4. Once these have been prepared, go to the video and press play.
5. The data sheet is set up for every half a degree. To get the entirety of the degree, there will be an overshoot. The initial start of a the half a degree will start a 0.1 of the temperature you are on. Then you continue to watch until the very end of 0.5 - right up until it turns to 0.6.
    a. It will work the same way for the next increment. The start of 0.6 until the very end of 0.0 up until it changes to 0.1.
    b. This makes sure that you have all of that half a degree for that data point rather than just a partial of it. Think of it as time. If the video is stopped when the video turns to 0.5, you are getting the first 15 seconds of a 60 second moment. If you wait till the end, you will have the full 60 seconds applied.
6. Once all droplets are frozen and all the droplets have been recorded in the spreadsheet, fill in the rest of the rows in the column with the total number of droplets.
    a. This is so that the entire spreadsheet is filled out with the proper information.
7. Save the spreadsheet and email the file to your supervisor